Neural Circuit for Locust Flight

2013/01/10

Tatsuo Okubo

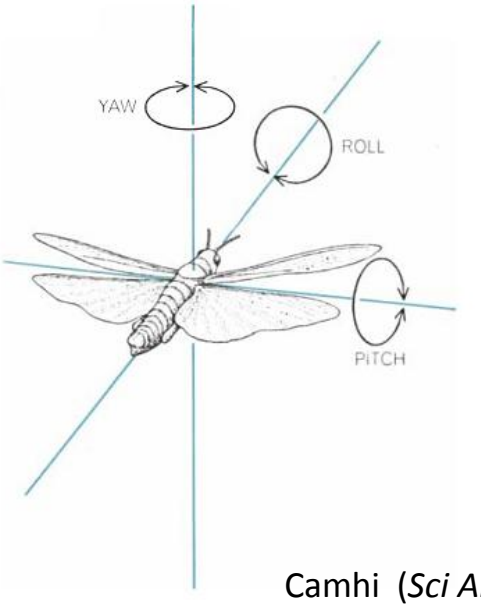

Camhi (*Sci Am*, 1971)

http://www.youtube.com/watch?v=88SulH7Qvdo

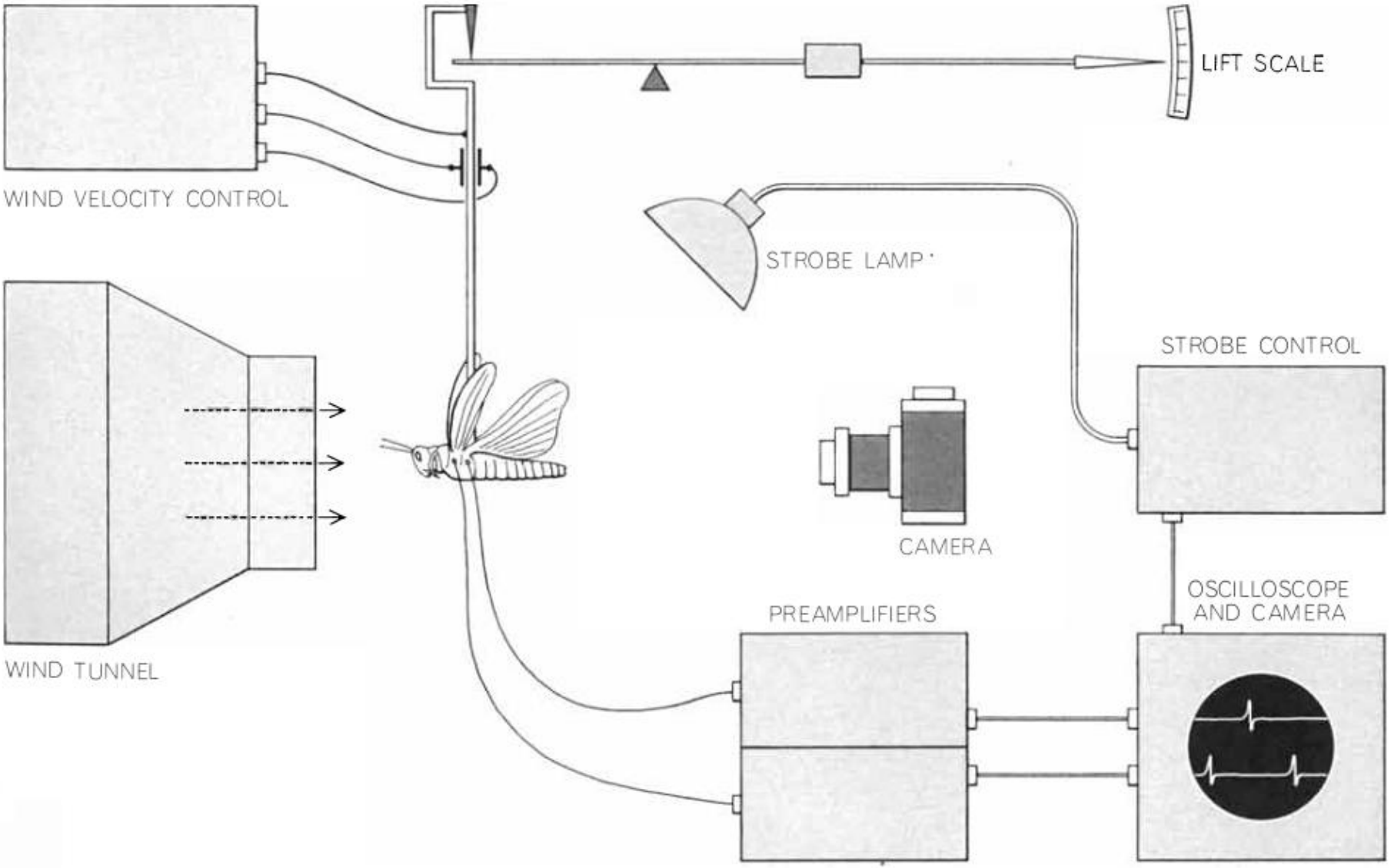

Wilson DM (*Sci Am*, 1968)

Locust in a wind tunnel

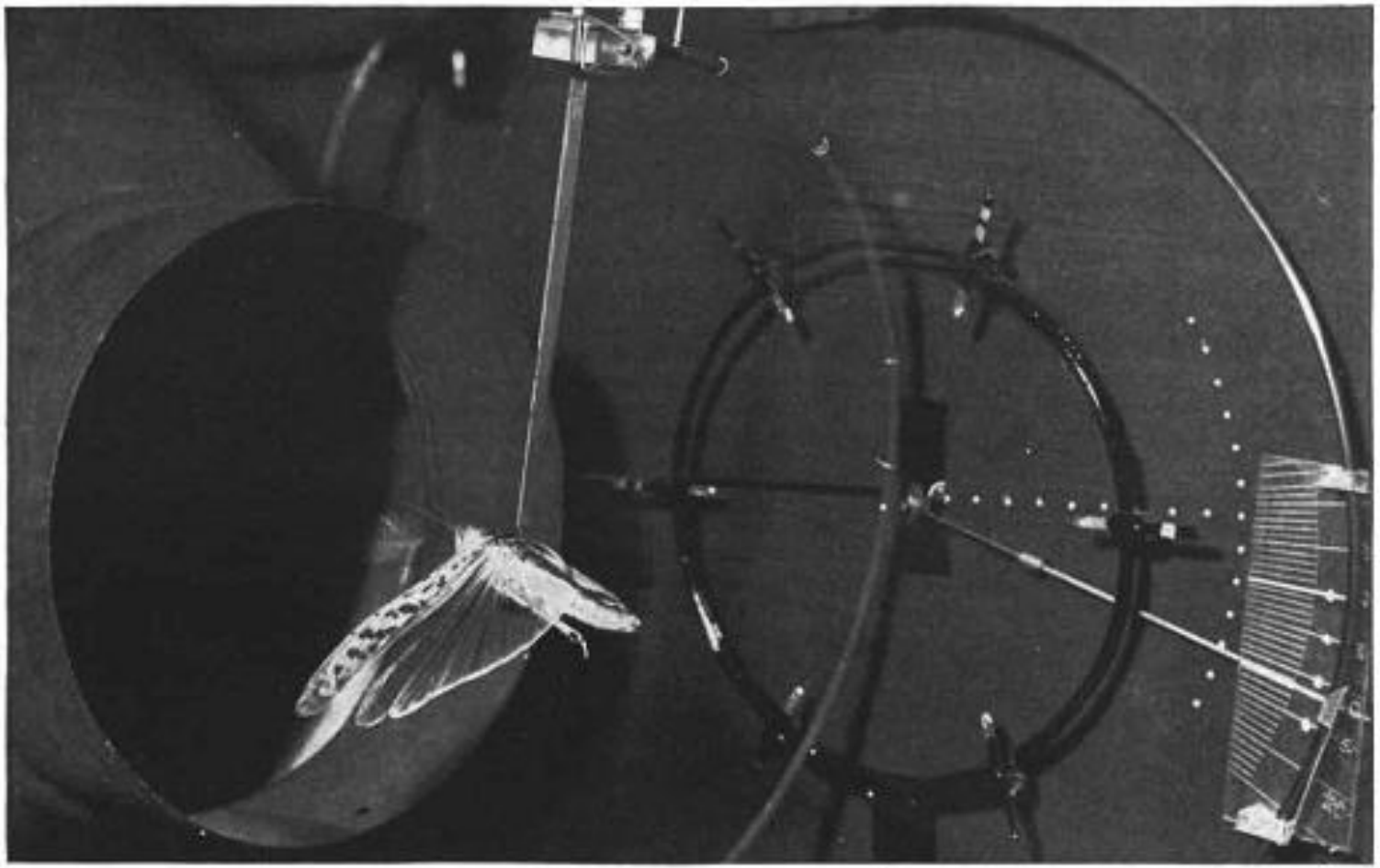

Weis-Fogh T (*Sci Am*, 1956)

Locust on a merry-go-round

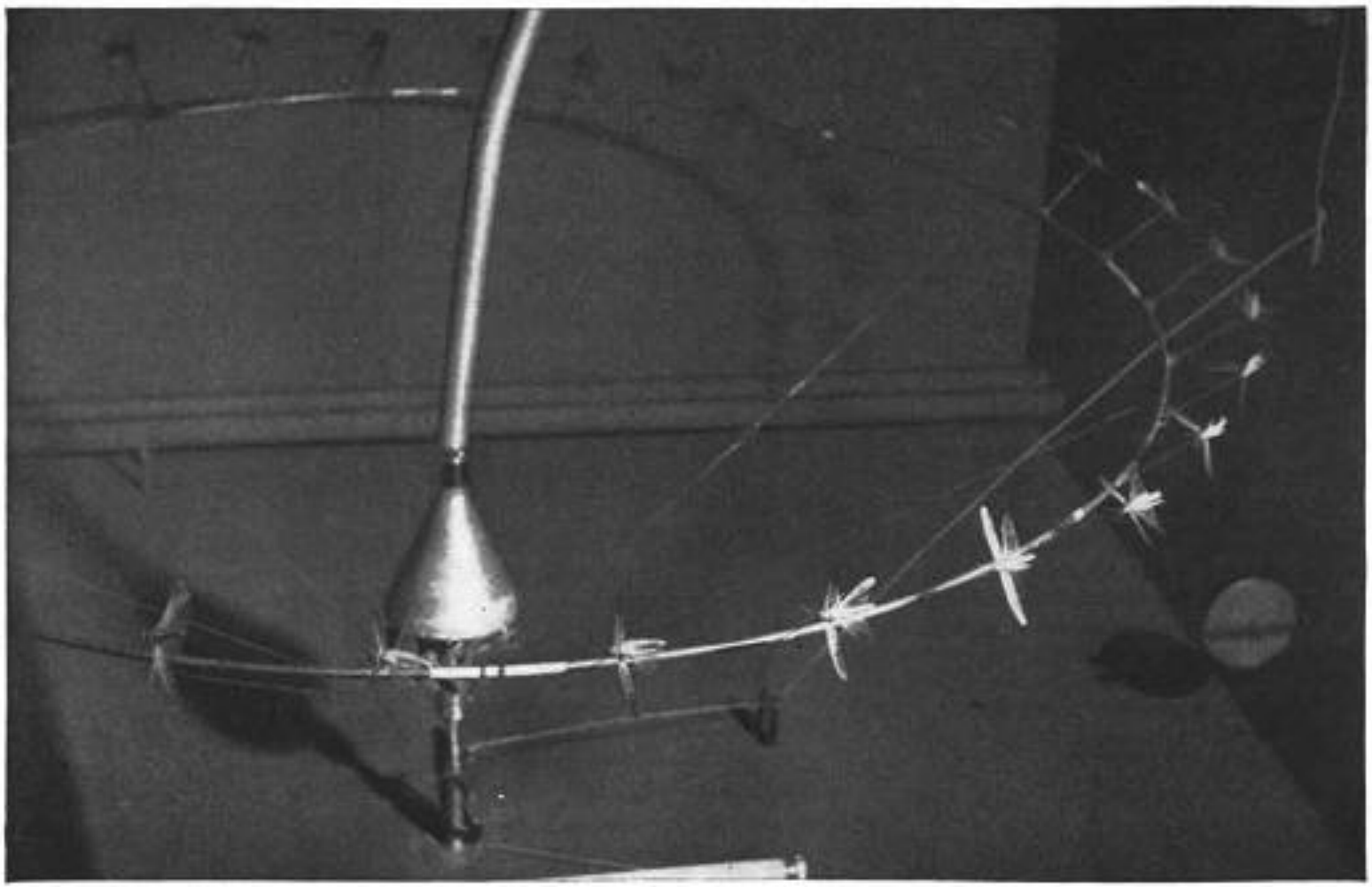

Weis-Fogh T (*Sci Am*, 1956)

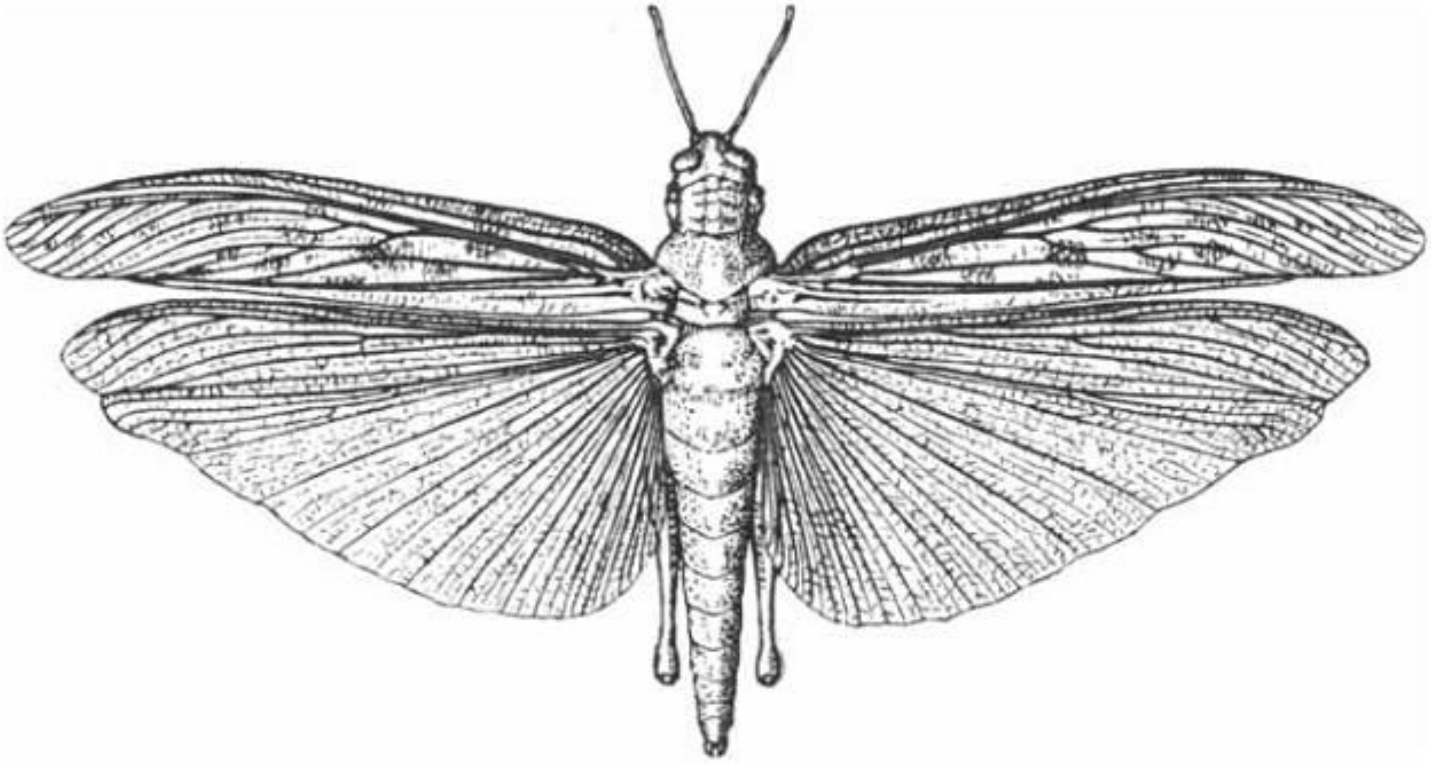

TOP VIEW OF LOCUST shows its wings in outline. The forewings are stiff throughout, and their shape is completely under the insect's control. The hindwings are stiff in their forward part, but their rear halves are flexible and their shape is molded by the air stream.

Weis-Fogh T (*Sci Am*, 1956)

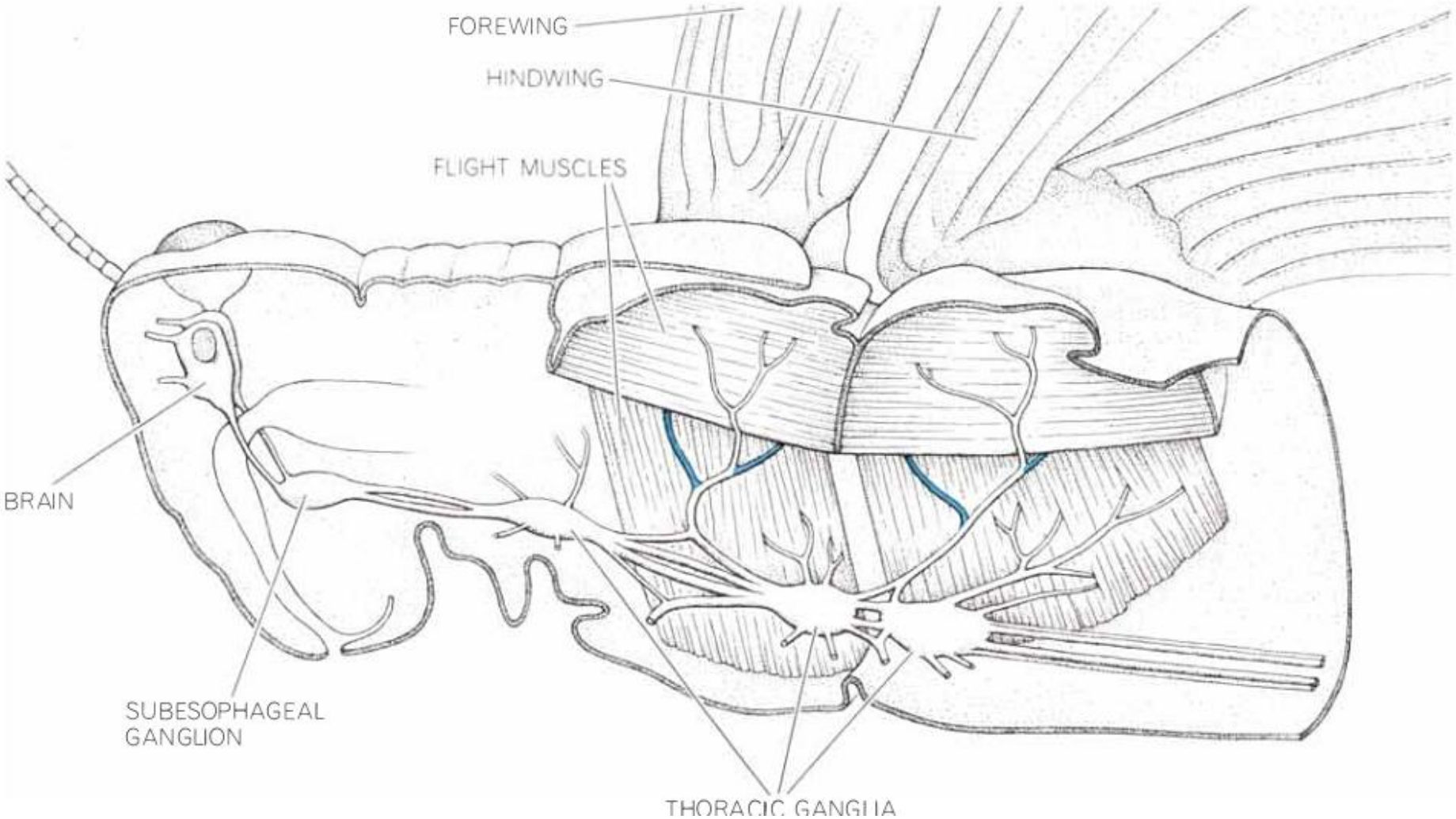

Wilson DM (*Sci Am*, 1968)

EMG recordings during free flight!

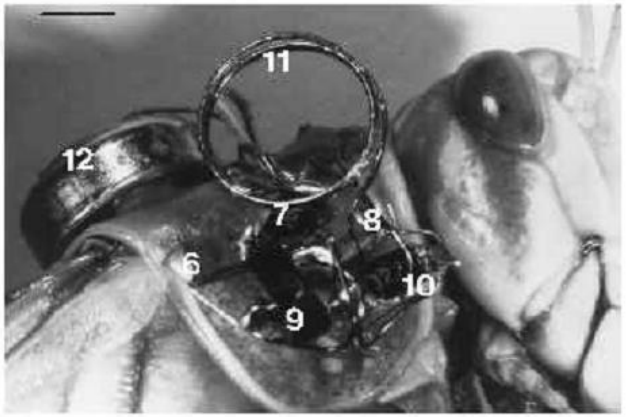

Fig. 2. Photograph of head and prothoracic shield of *Schistocerca gregaria* showing part of the transmitter–modulator circuit. For identification of components, see Fig. 1A. Scale bar, 2 mm.

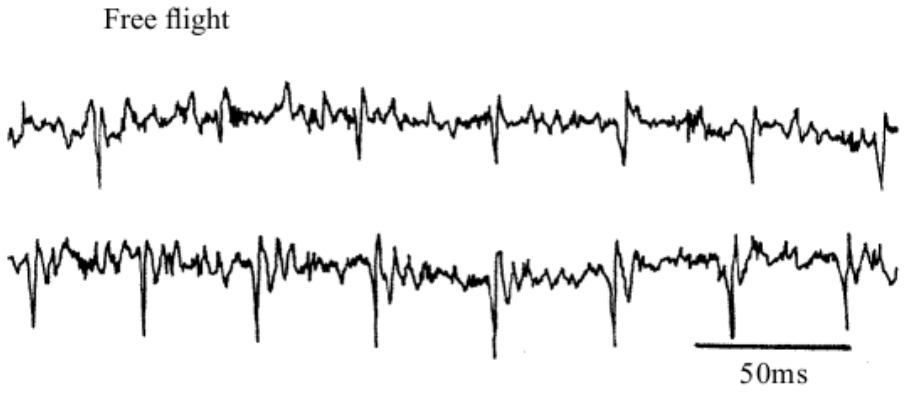

Fig. 4. Transmission of muscle potentials (M129) during two sequences of free flight from two different female *Schistocerca gregaria*.

Kutsch et al. (J Exp Biol, 1993)

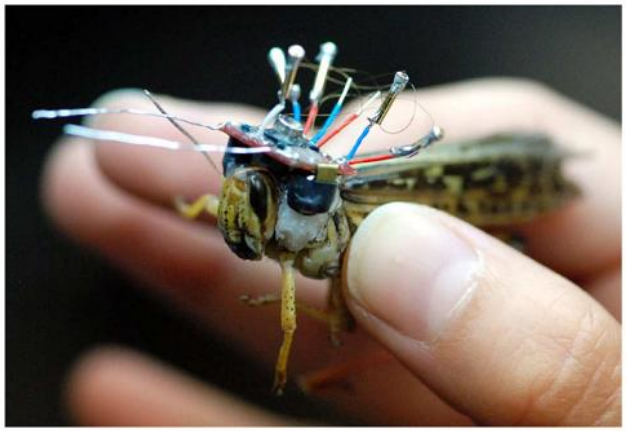

Fig. 7. Version 1 telemetry system mounted on a locust *Schistocerca americana*.

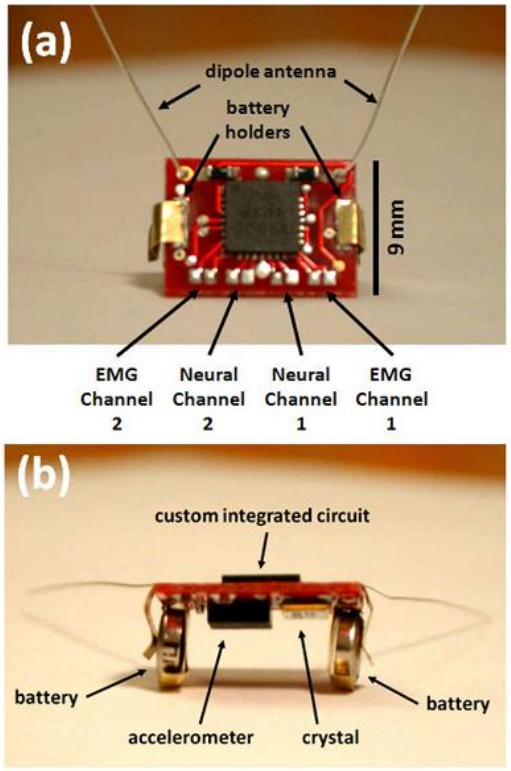

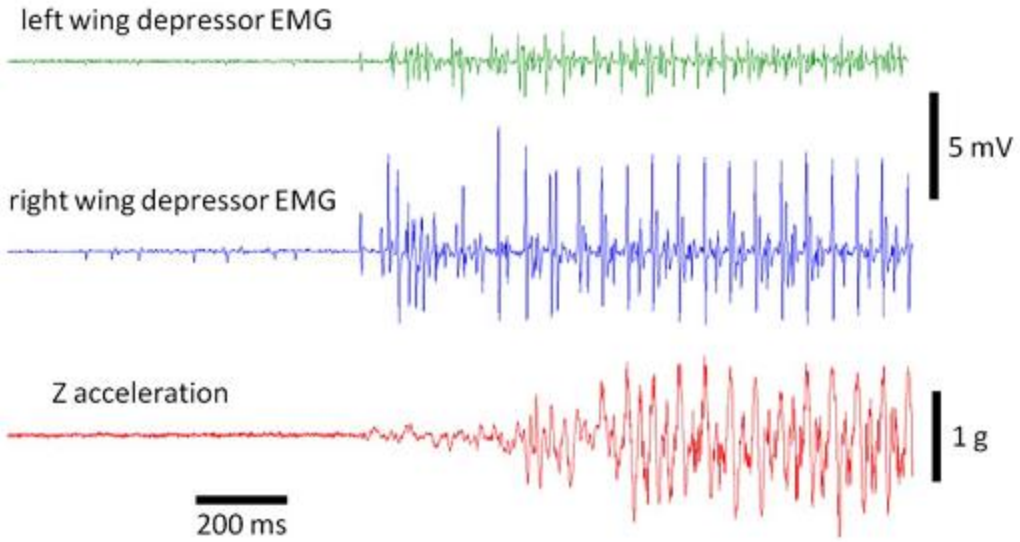

Fig. 10. Data obtained wirelessly from a loosely tethered locust flying in a wind tunnel. The onset of 18-Hz wing beats is observed in the two wing EMG traces (top) and acceleration trace (bottom).

Harrison et al. (*IEEE*, 2011)

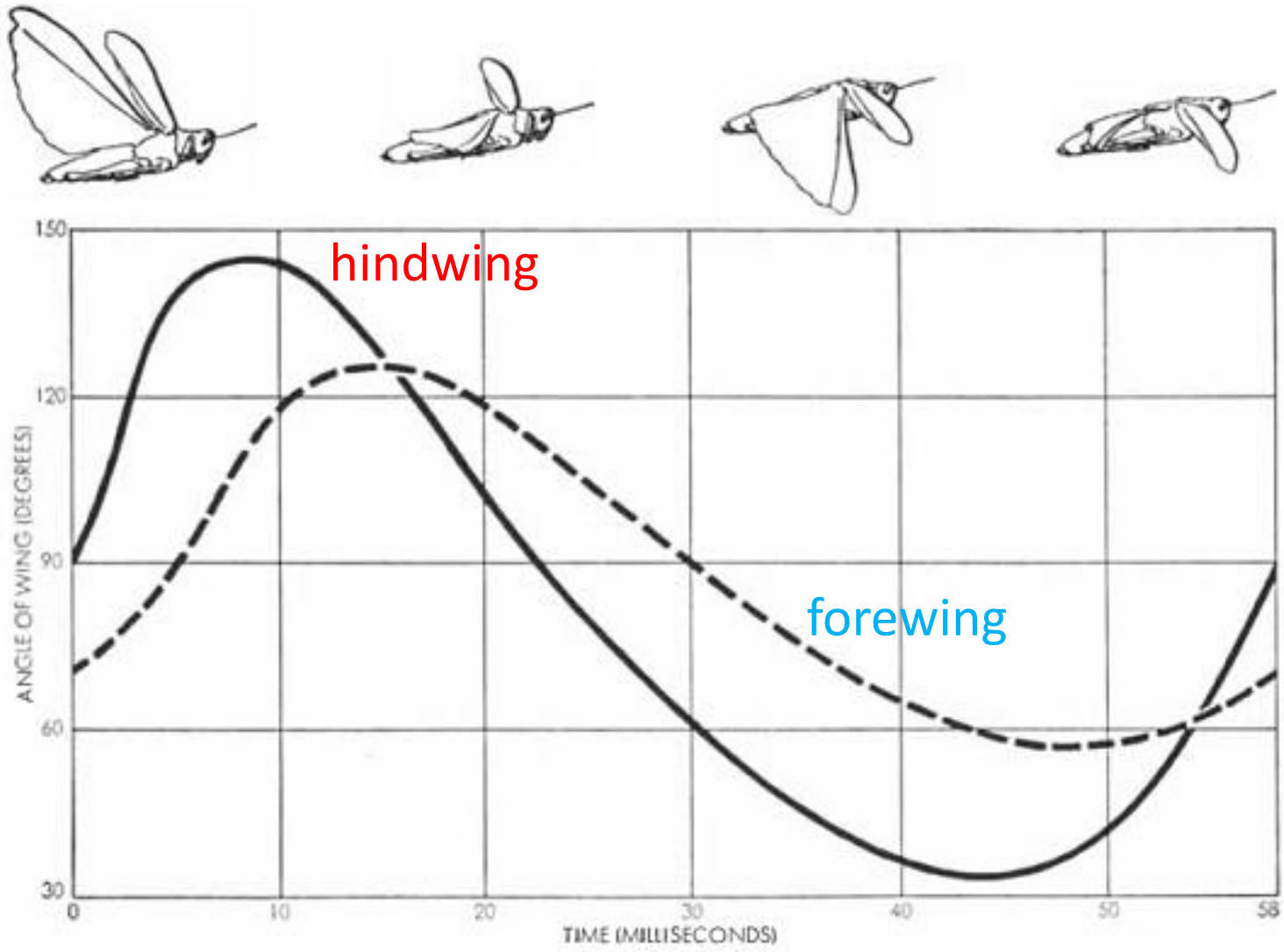

Weis-Fogh T (*Sci Am*, 1956)

Simultaneous EMG during fictive flight

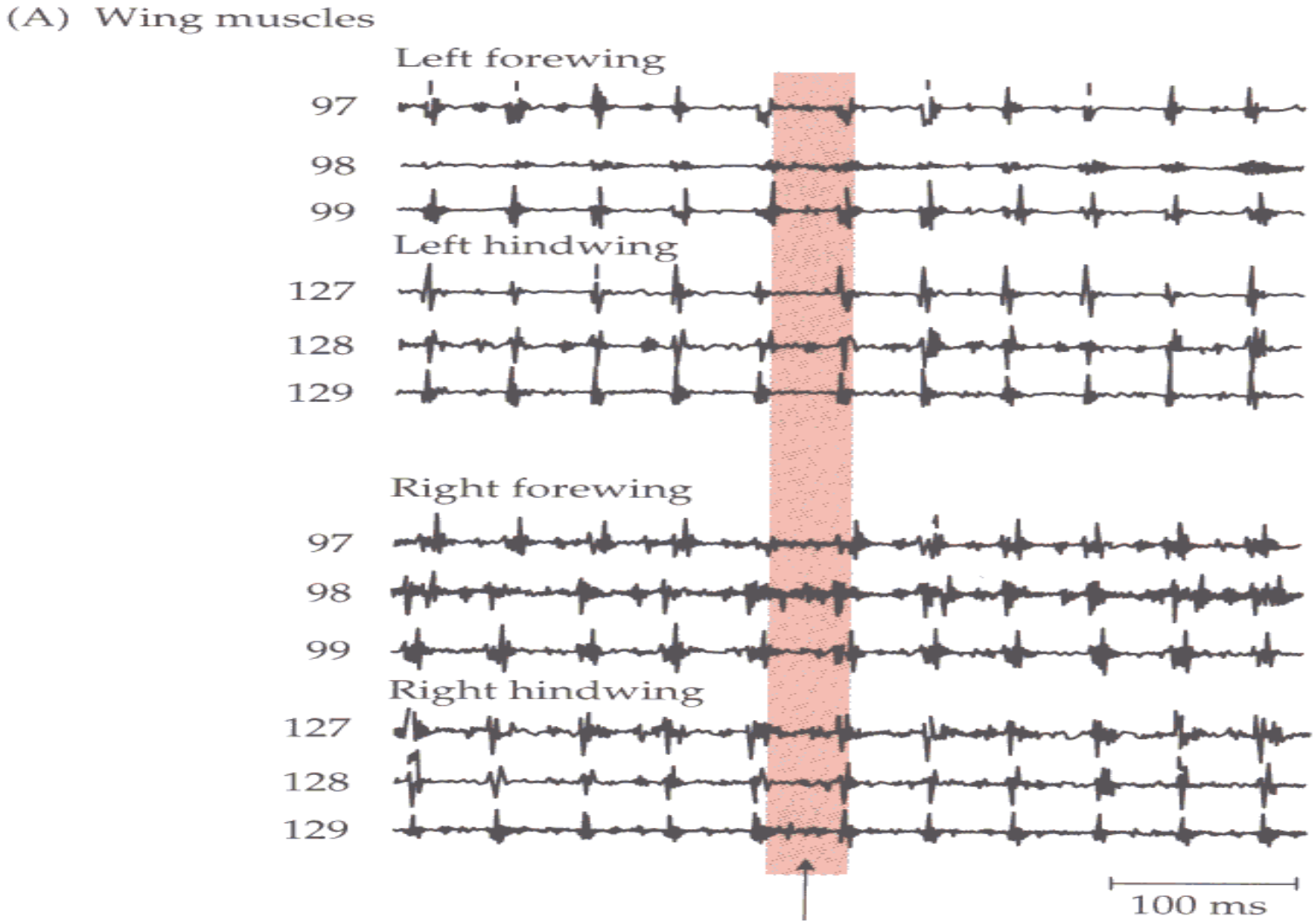

Zarnack & Möhl (*J Comp Physiol A*, 1977)

Locust nervous system

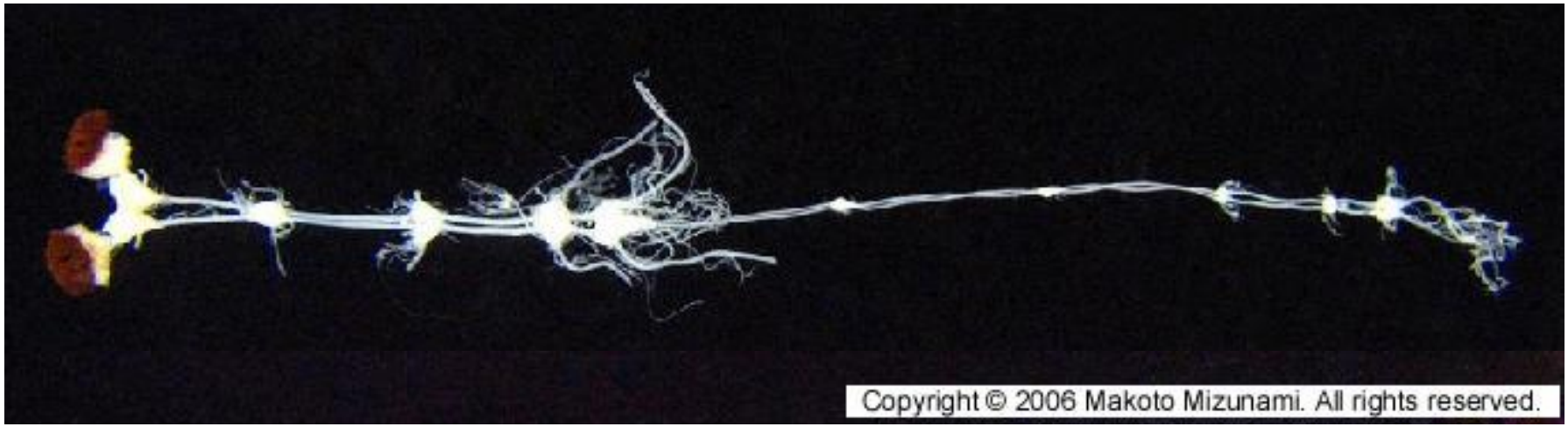

brain SOG thoracic abdominal

http://invbrain.neuroinf.jp/modules/newdb1/extract/7/thumbnail/img1/bata_zen.jpg

Intracellular recording during tethered flight

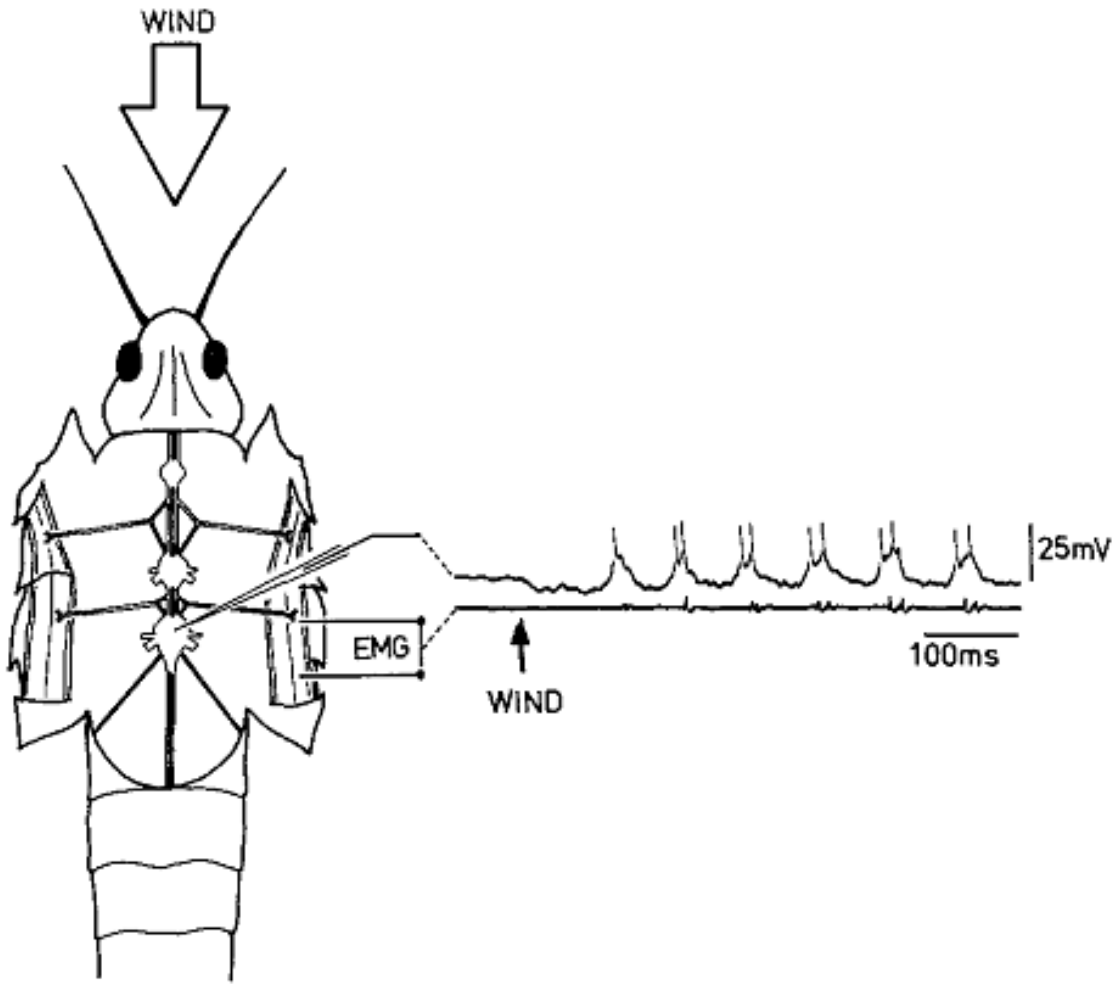

Robertson & Pearson (*J Comp Physiol A*, 1982)

Intracellular recording without deafferentiation

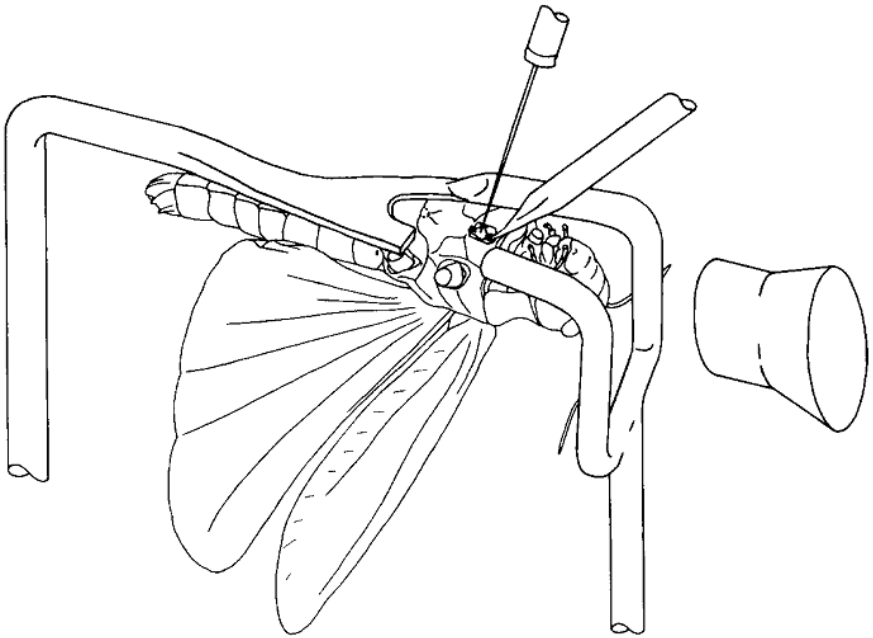

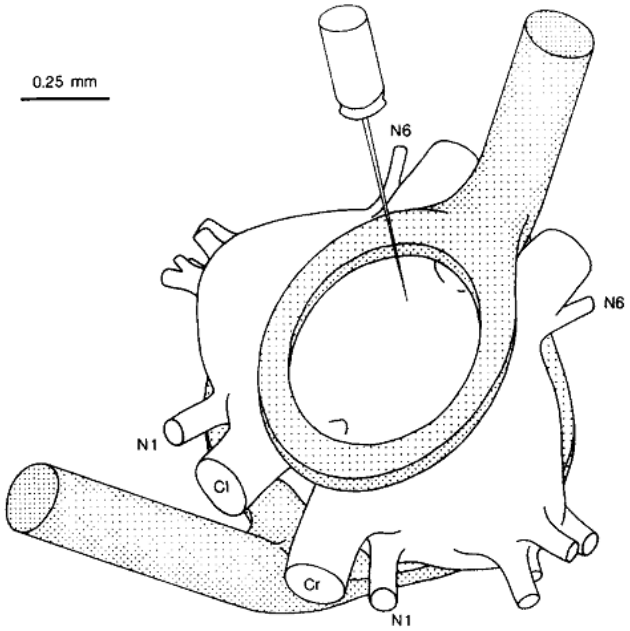

Wolf & Pearson (*J Neurosci Methods*, 1987)

Motor neurons are rhythmically active during fictive flight

Elevator MN

Depressor MN

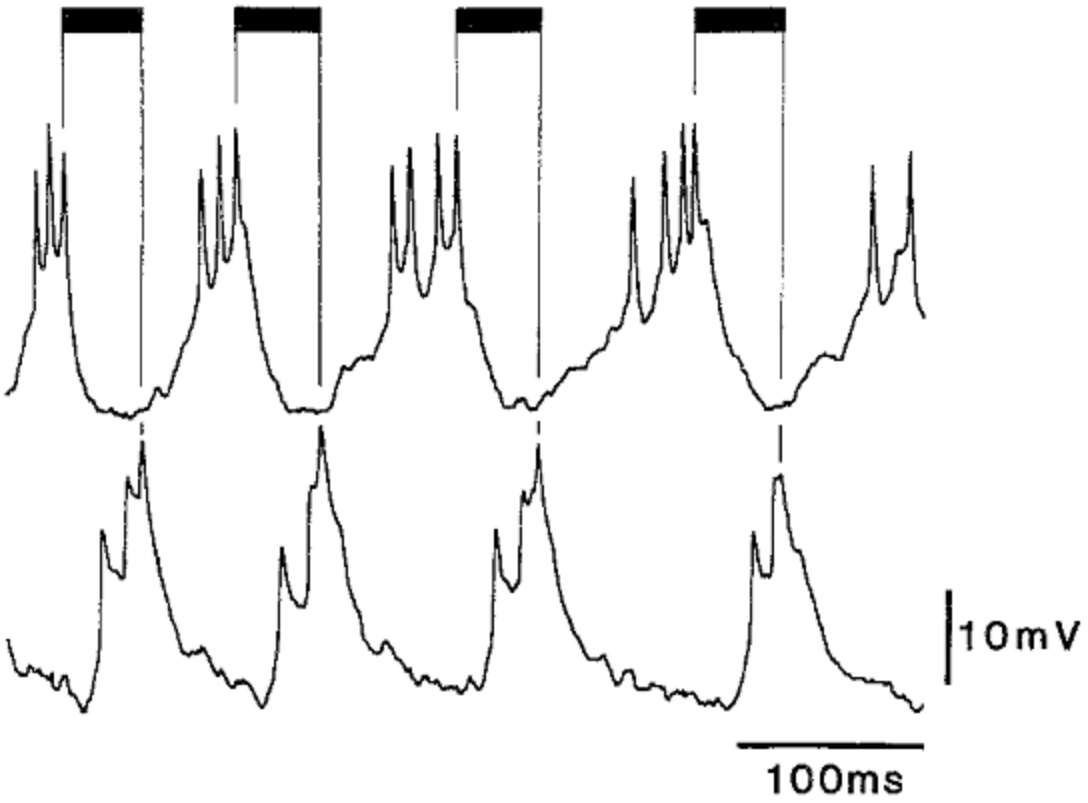

Hedwig & Pearson (*J Comp Physiol A*, 1984)

Hindwing depressor MN leads forewing depressor MN

forewing

hindwing

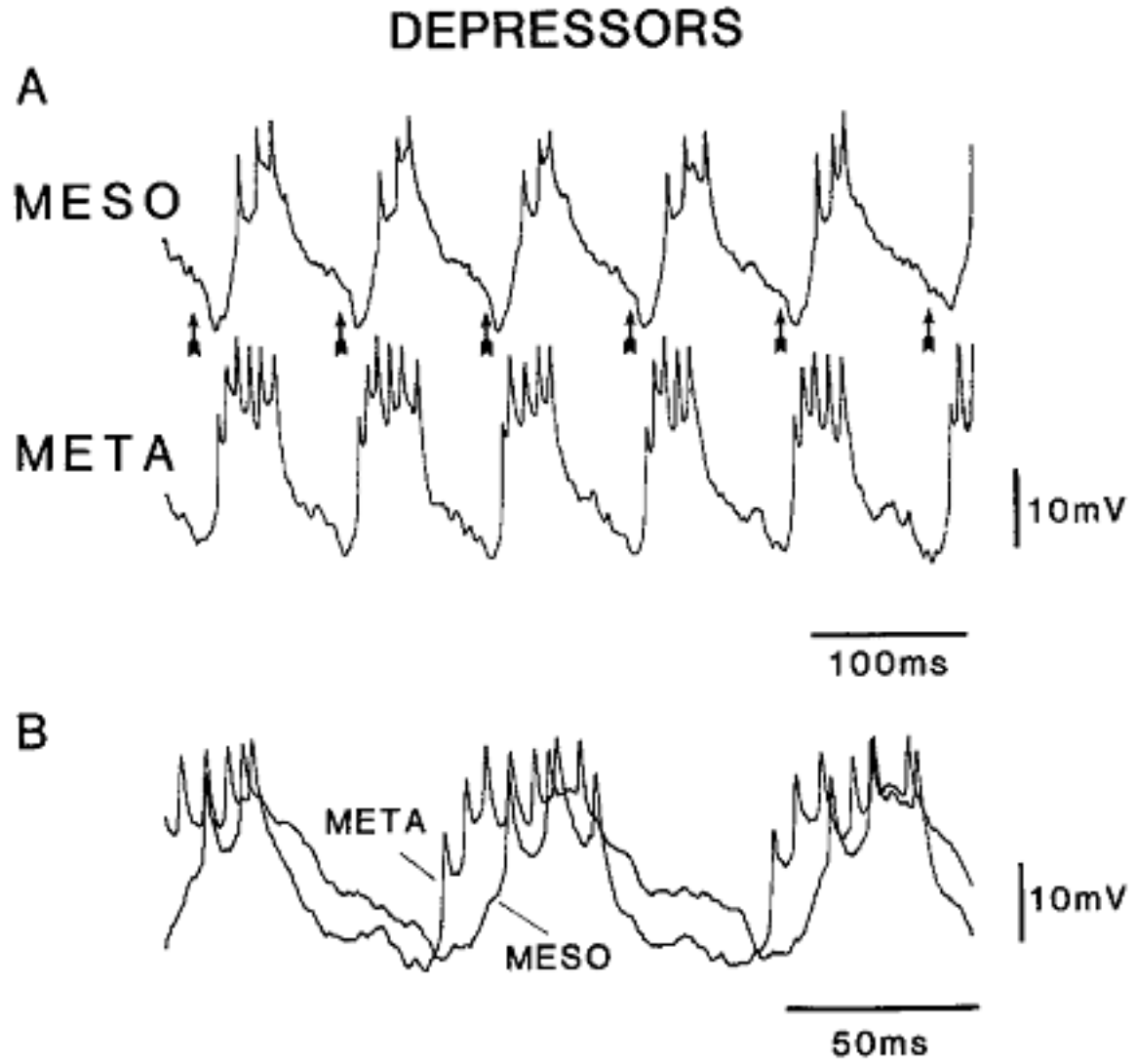

Hedwig & Pearson (*J Comp Physiol A*, 1984)

504 activates the elevator motor neuron

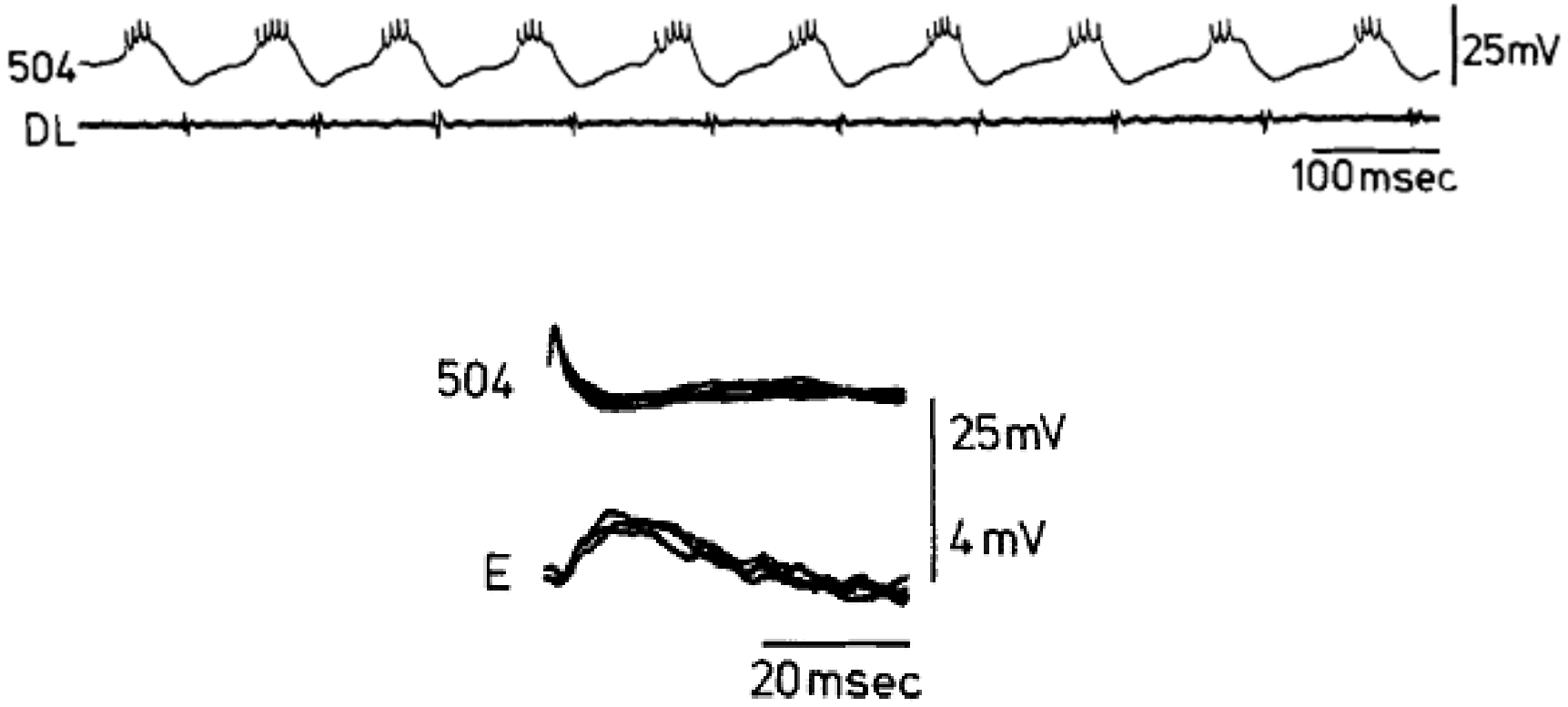

Robertson & Pearson (*J Comp Neurol*, 1983)

504 & 301

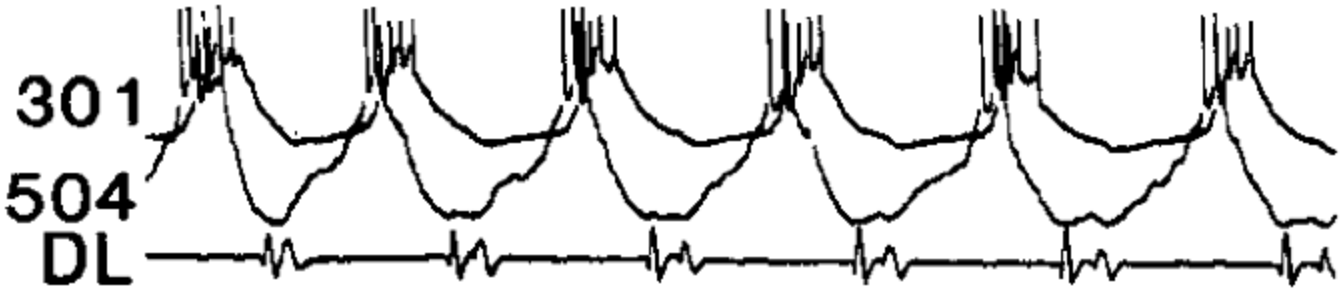

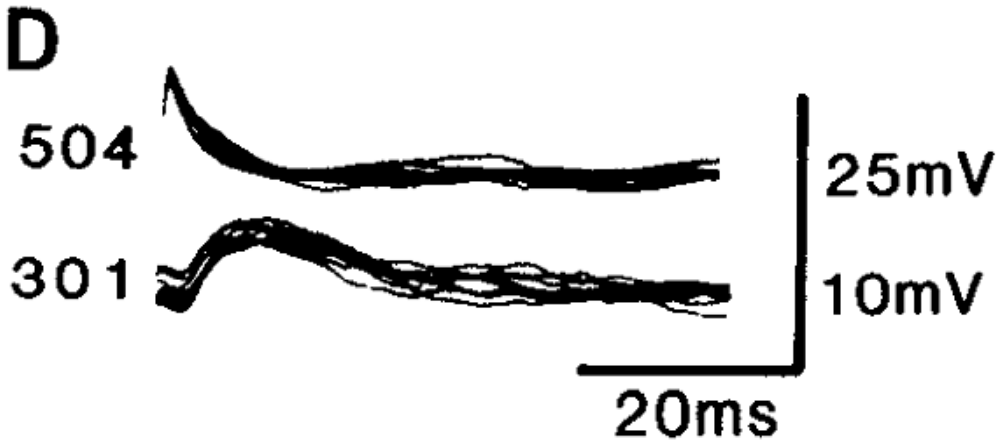

Robertson & Pearson (*J Neurophysiol*, 1985)

206 responds to wind and activates 504

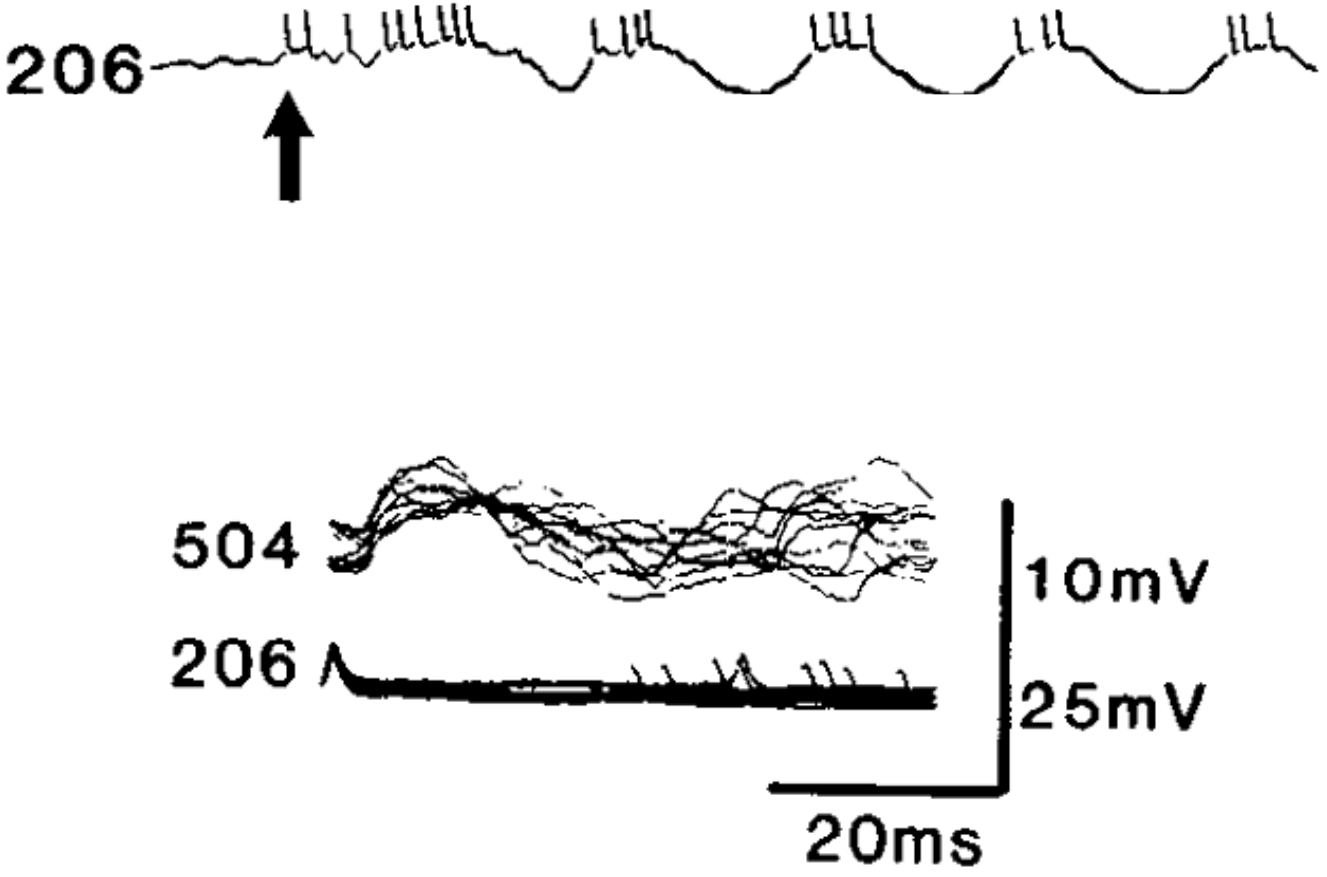

Robertson & Pearson (*J Neurophysiol*, 1985)

301 and 501 shows rhythmic activity during fictive flight

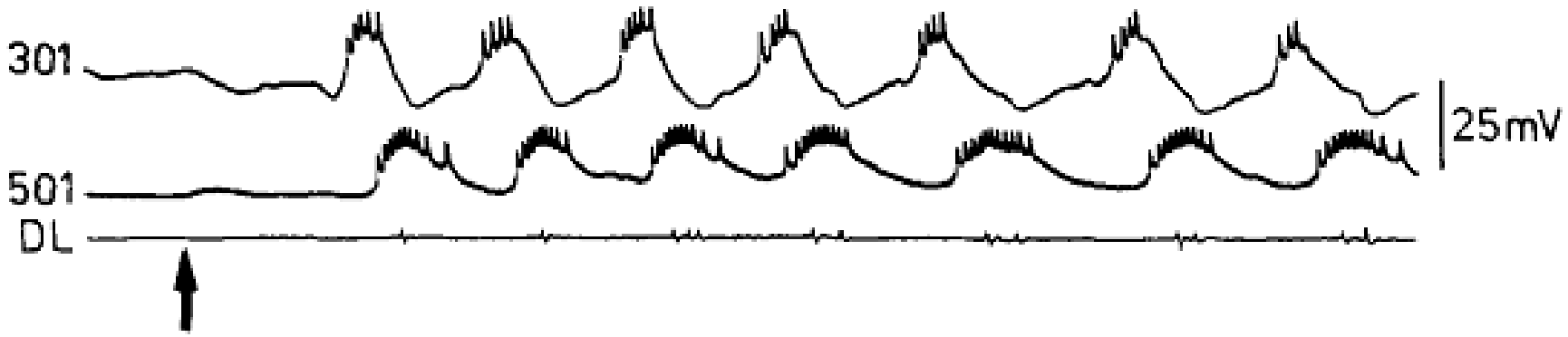

Robertson & Pearson (*J Comp Neurol*, 1983)

301 & 501 both pass the “reset” test

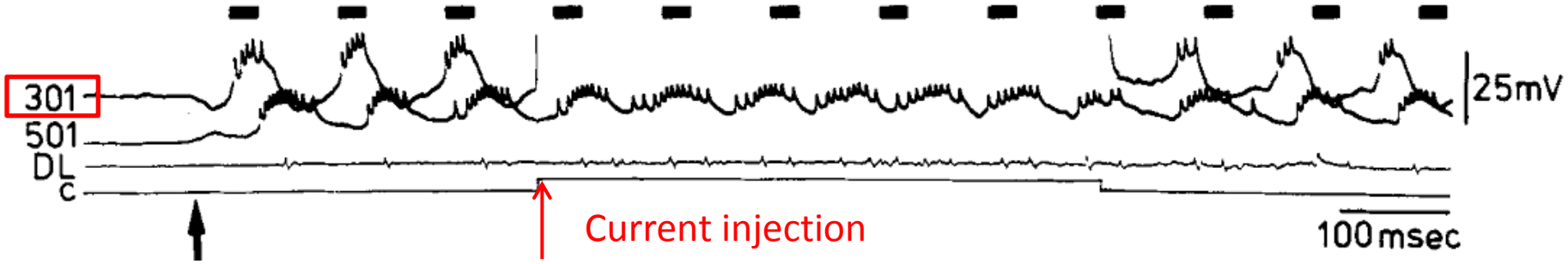

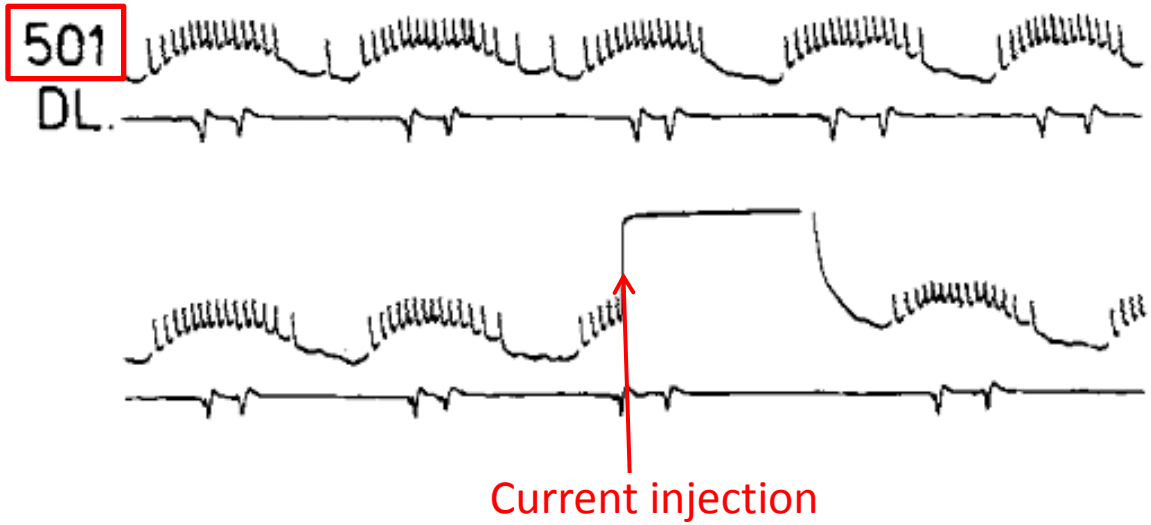

Robertson & Pearson (*J Comp Neurol*, 1983)

Interaction between 301 and 501

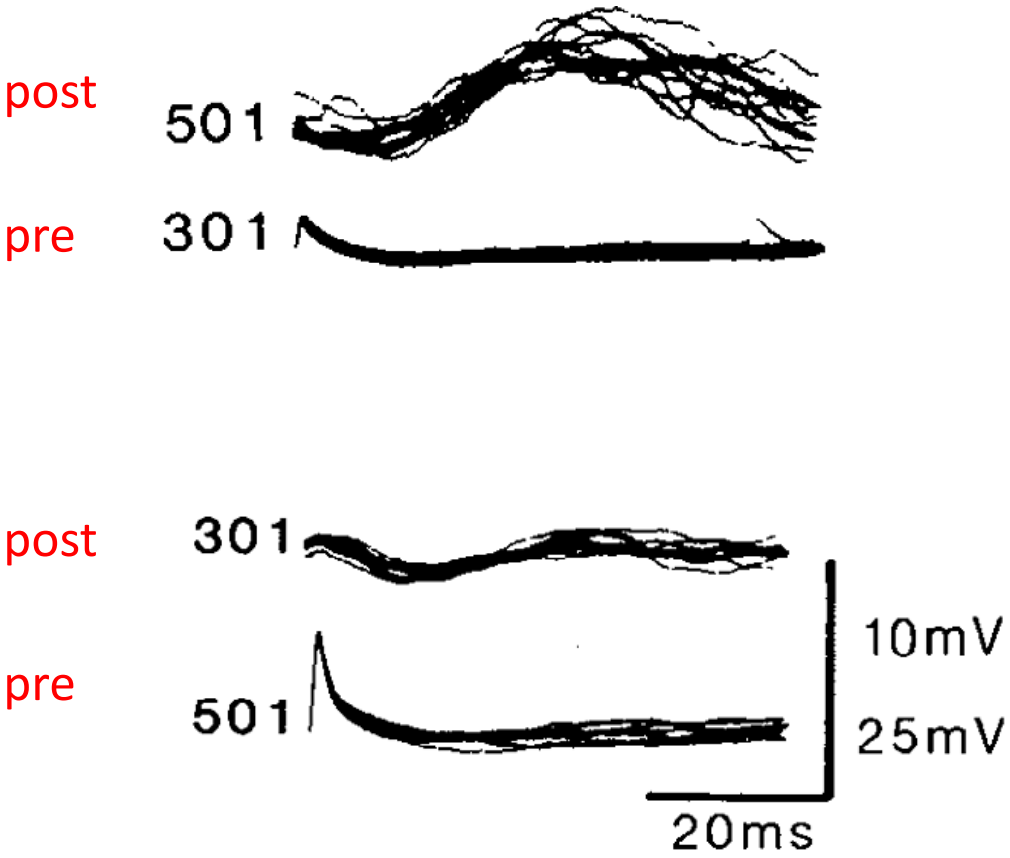

Robertson & Pearson (*J Neurophysiol*, 1985)

Delayed excitation is partly mediated by disinhibition

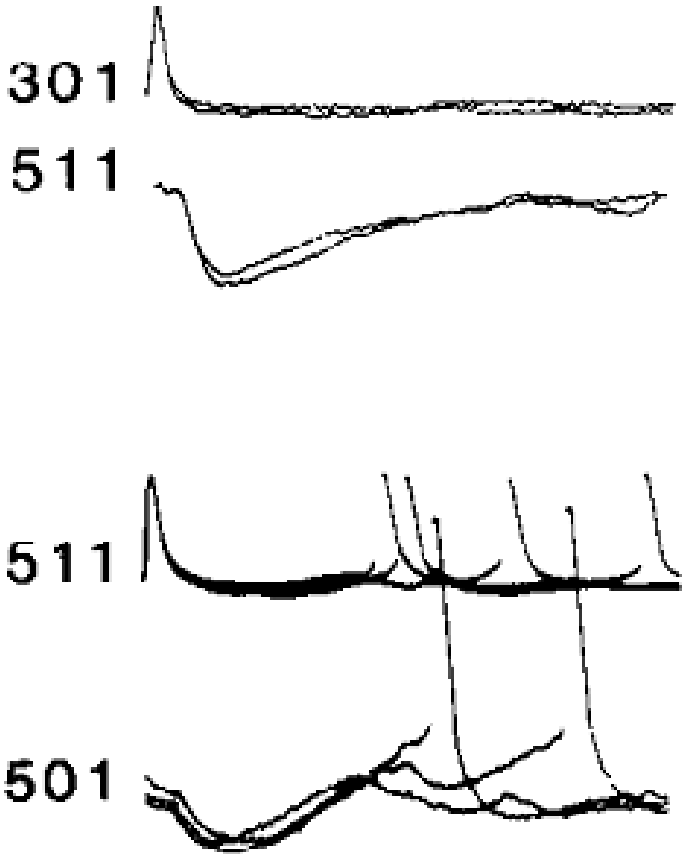

Robertson & Pearson (*J Neurophysiol*, 1985)

And finally…

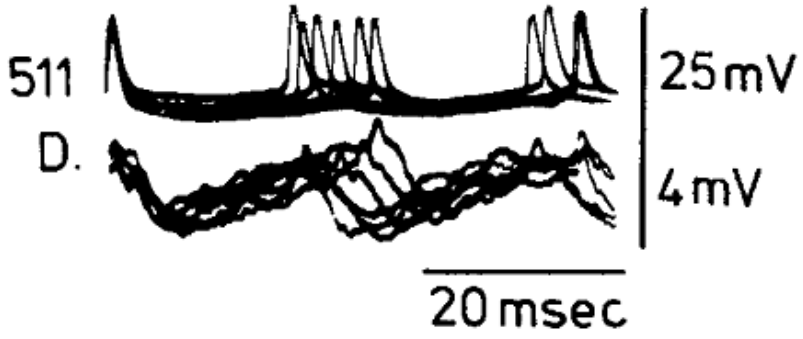

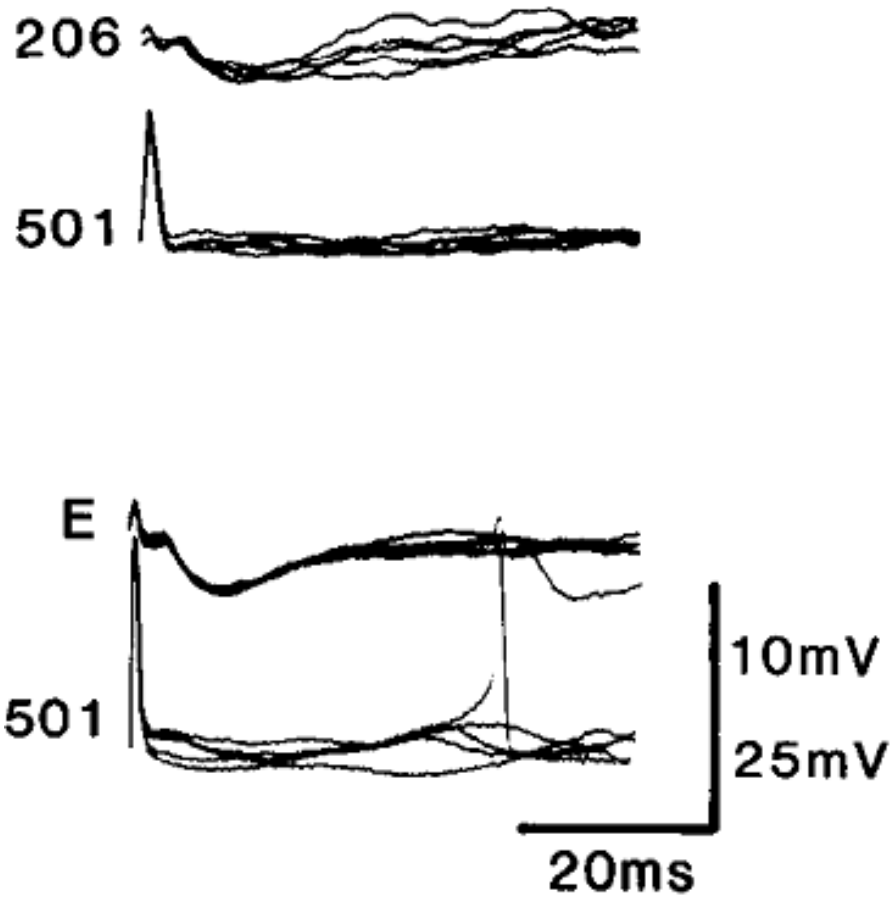

Time to simulate the circuit on a computer!

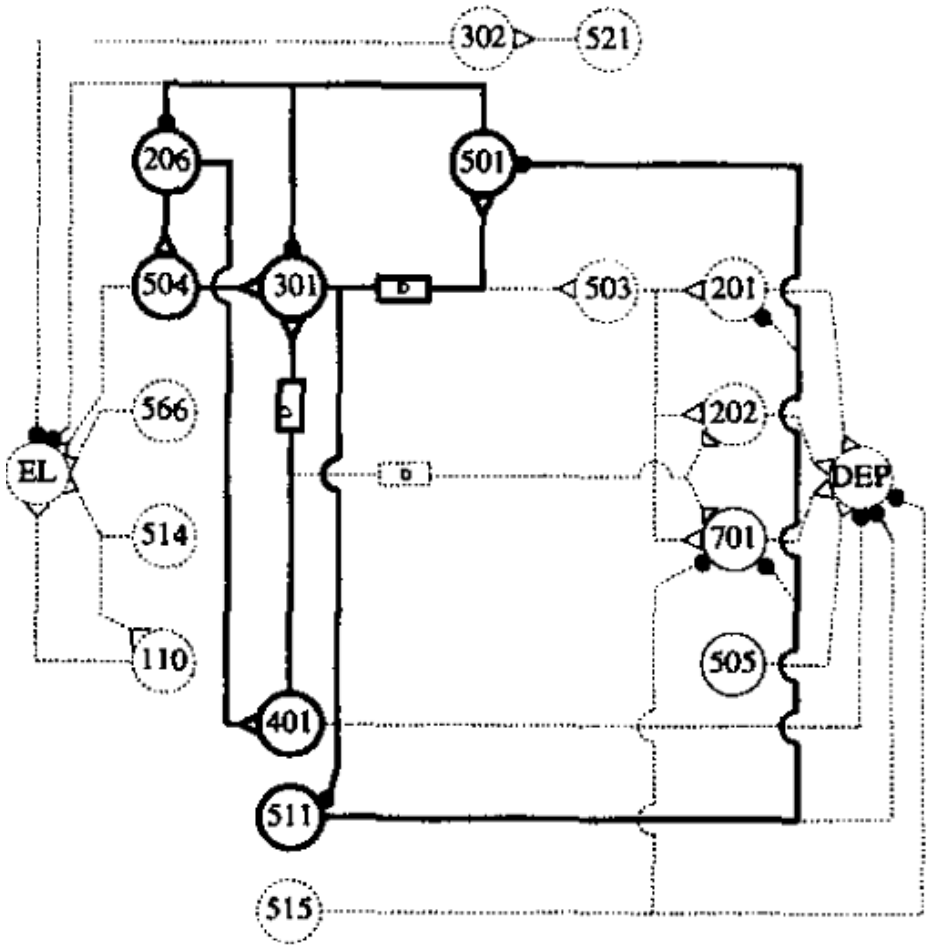

Grimm & Sauer (*Biol Cyber*, 1995)

Activity of flight interneuron 301

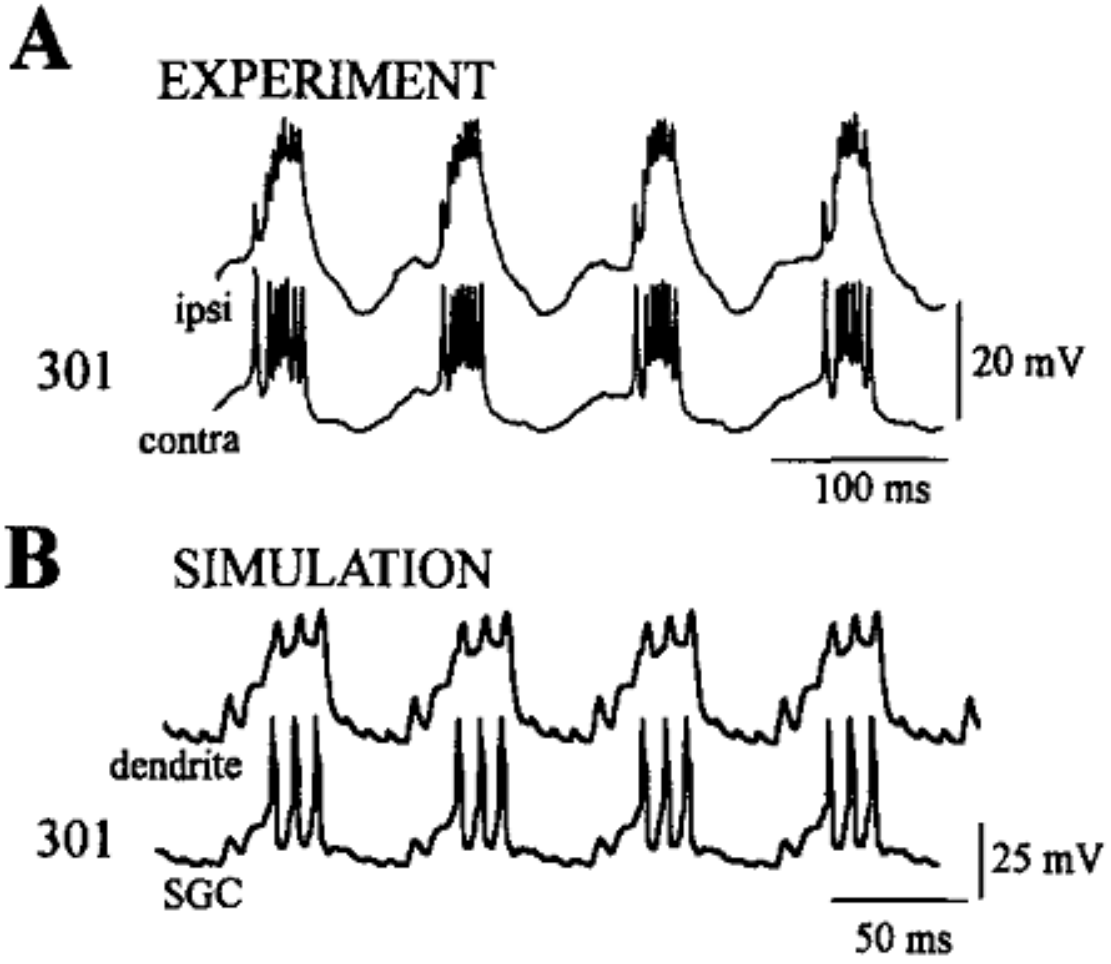

Grimm & Sauer (*Biol Cyber*, 1995)

Rhythmic pattern is reproduced

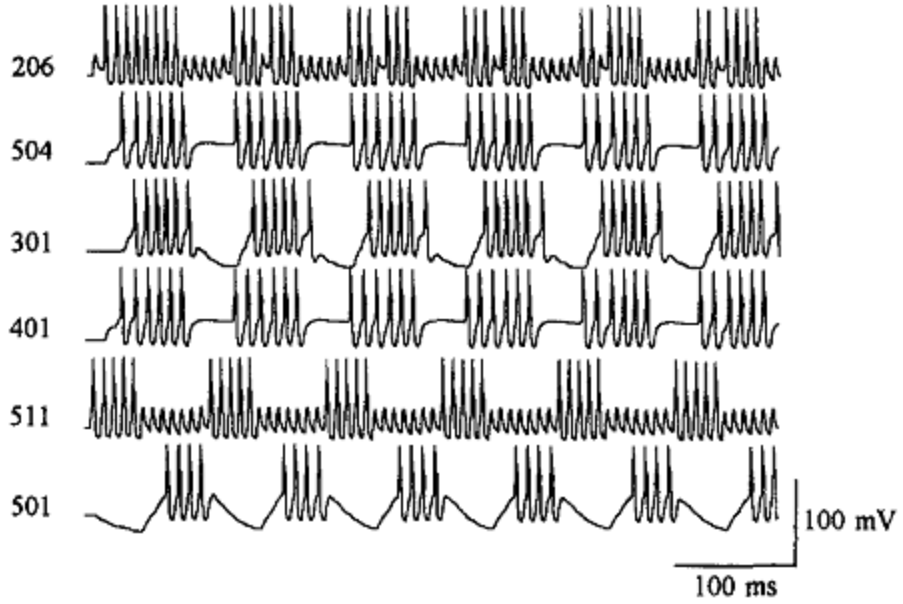

Experiment

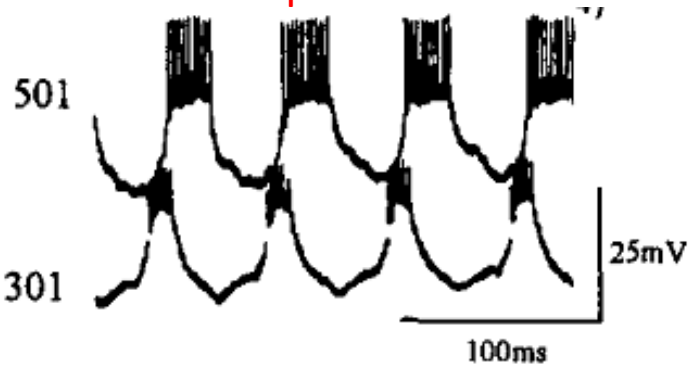

Simulation

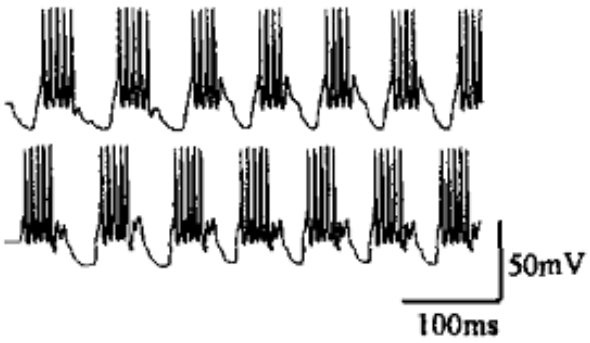

Grimm & Sauer (*Biol Cyber*, 1995)

(1) Wing hinge stretch receptors

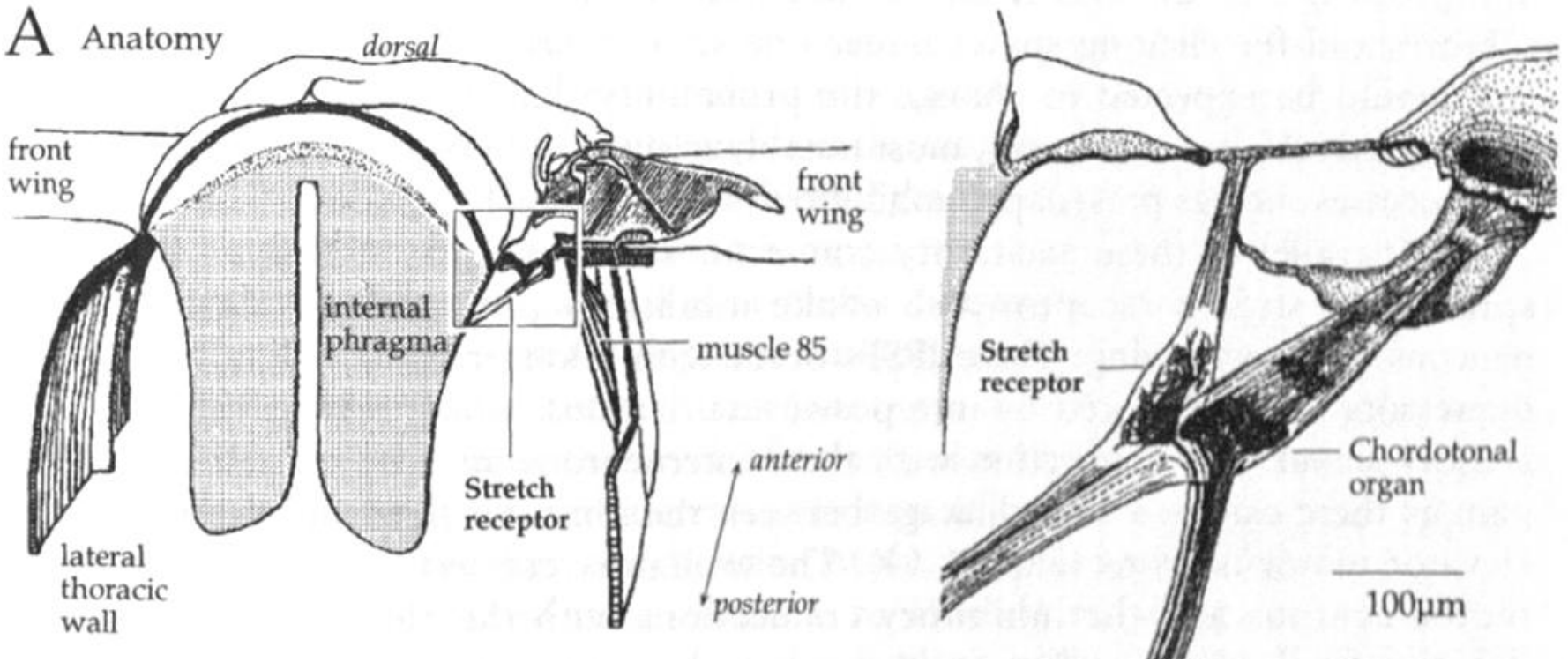

Burrows (1996)

Wing hinge receptors activate depressor motor neurons

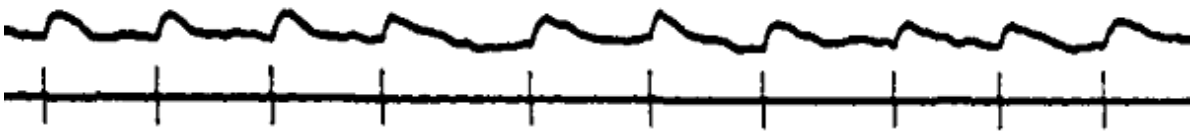

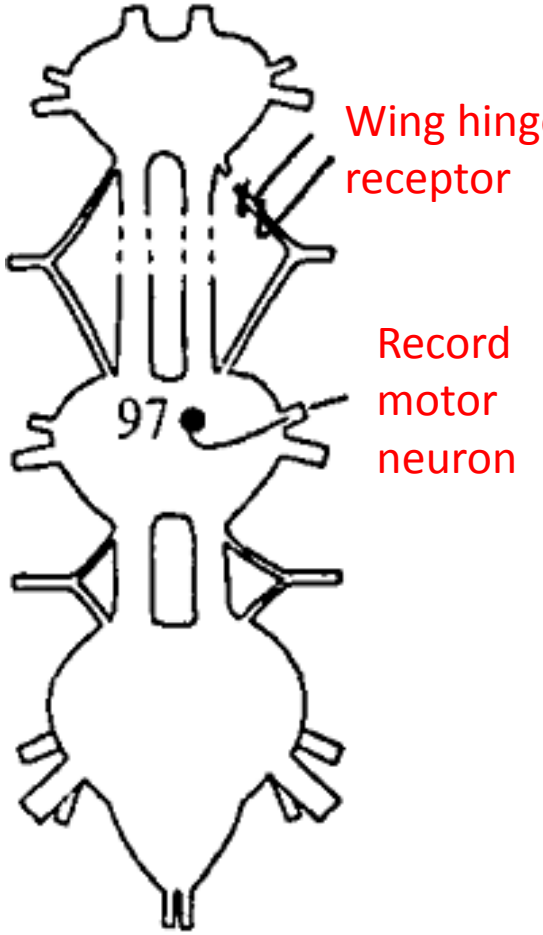

Burrows (*J Exp Biol*, 1975)

(2) Tegula

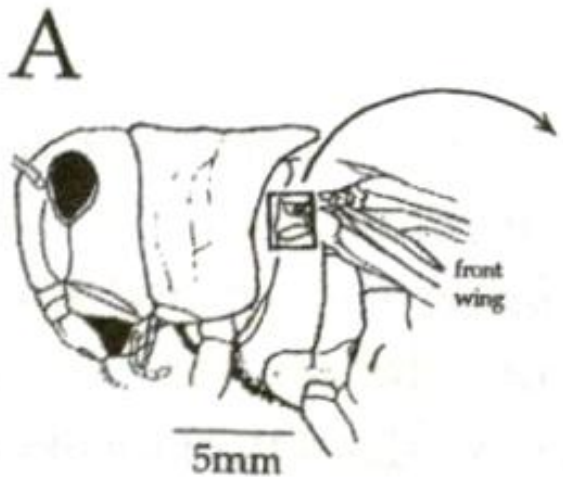

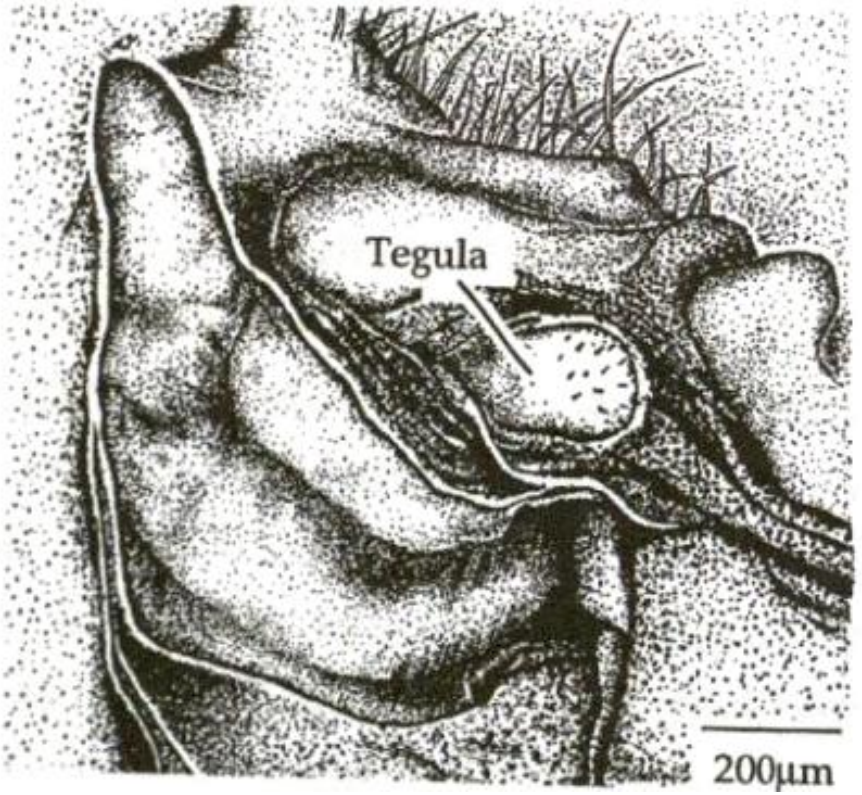

Burrows (1996)

(3) Campaniform sensilla

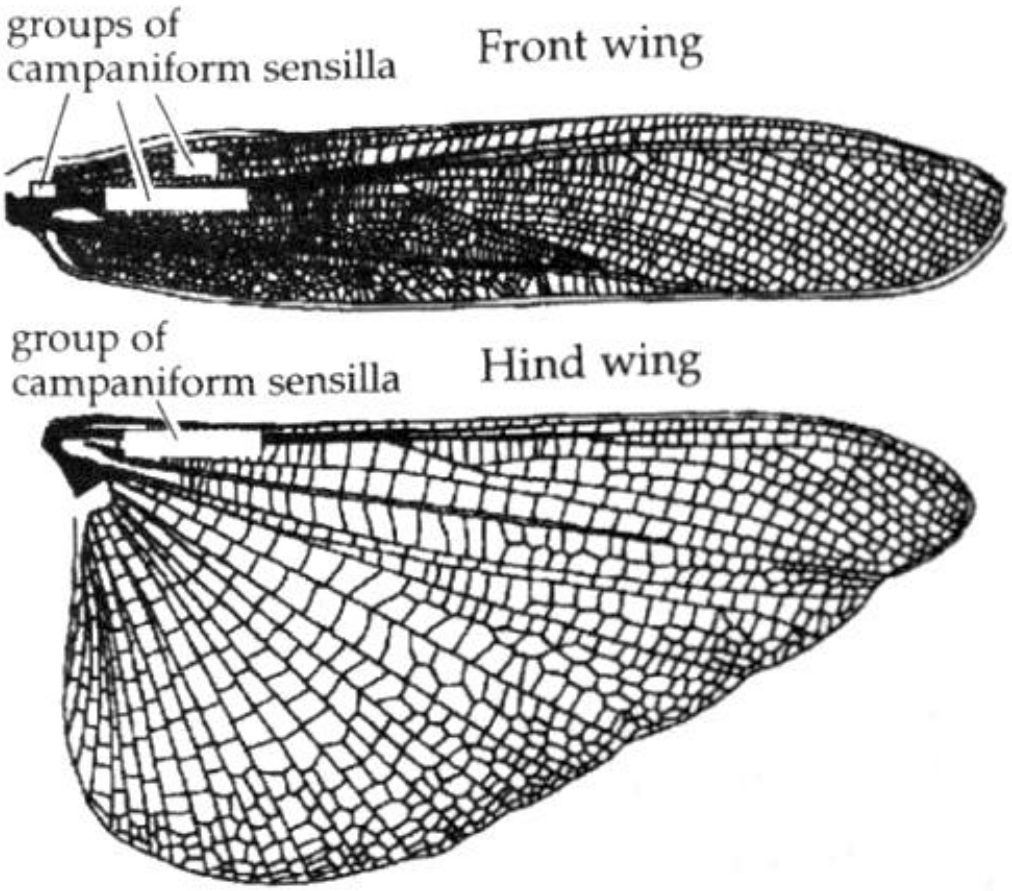

Burrows (1996)

How do locusts maintain a stable flight?

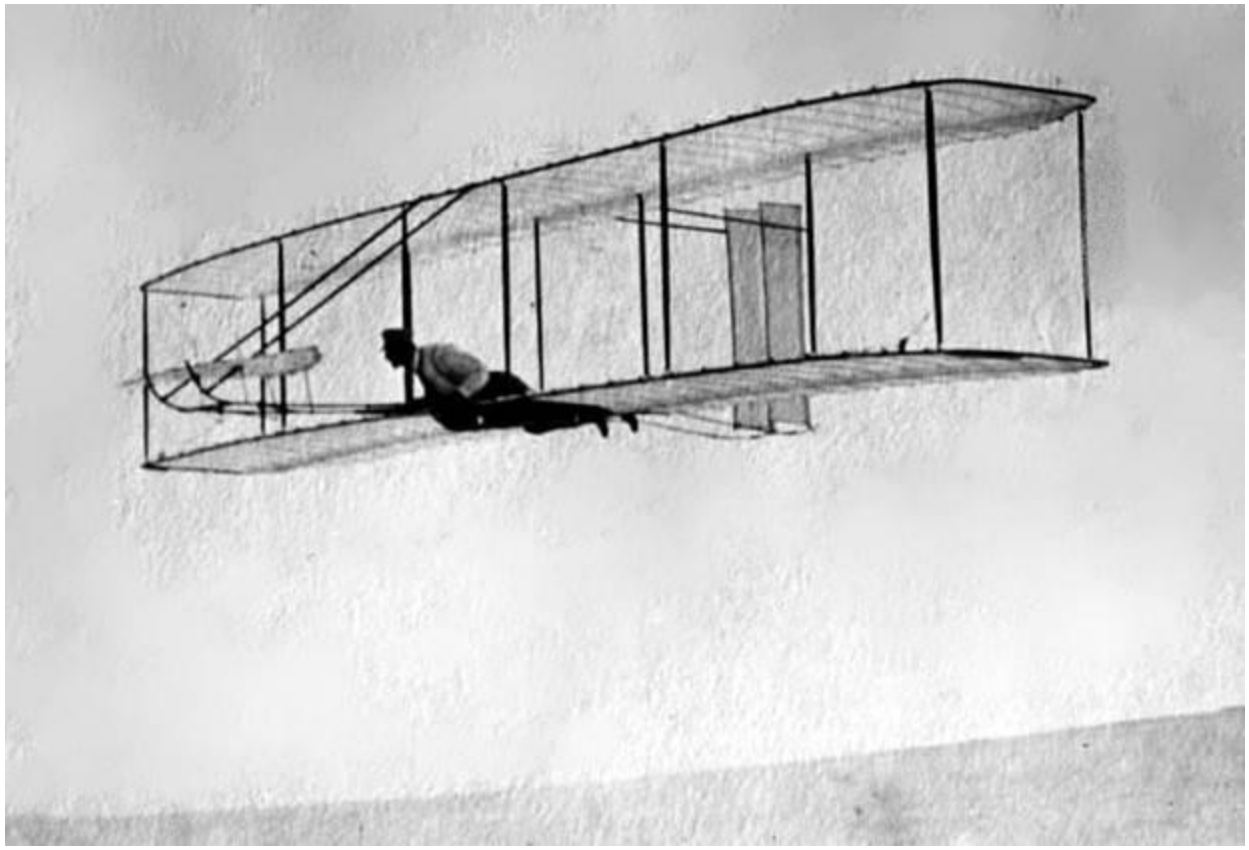

Multiple sensory organs for detecting deviation

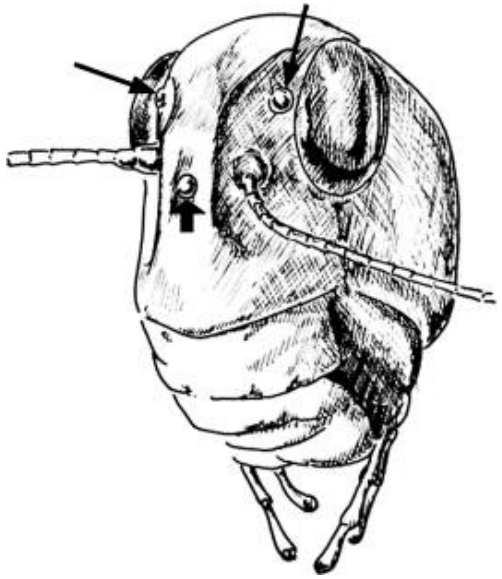

Berry et al. (*Vision Research*, 2007)

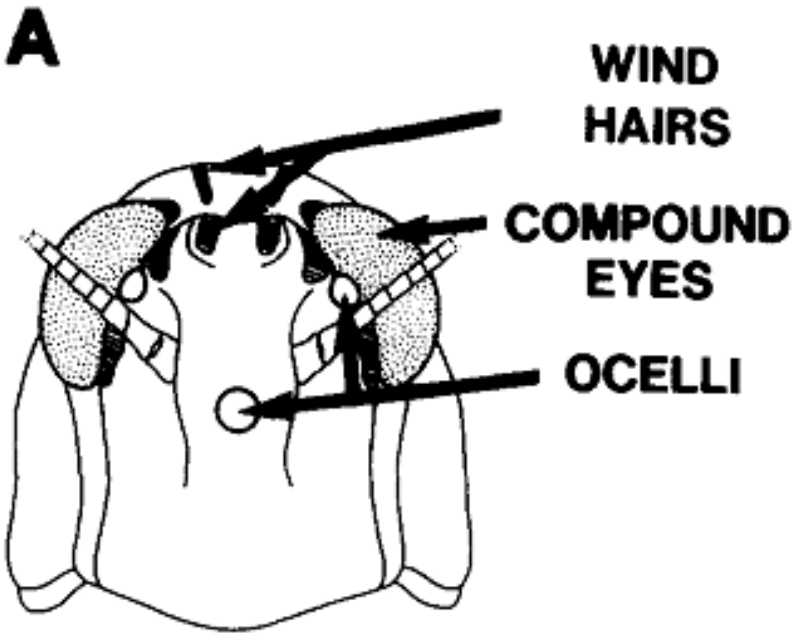

Reichert & Rowell (*TINS*, 1986)

Ocelli can detect the horizon

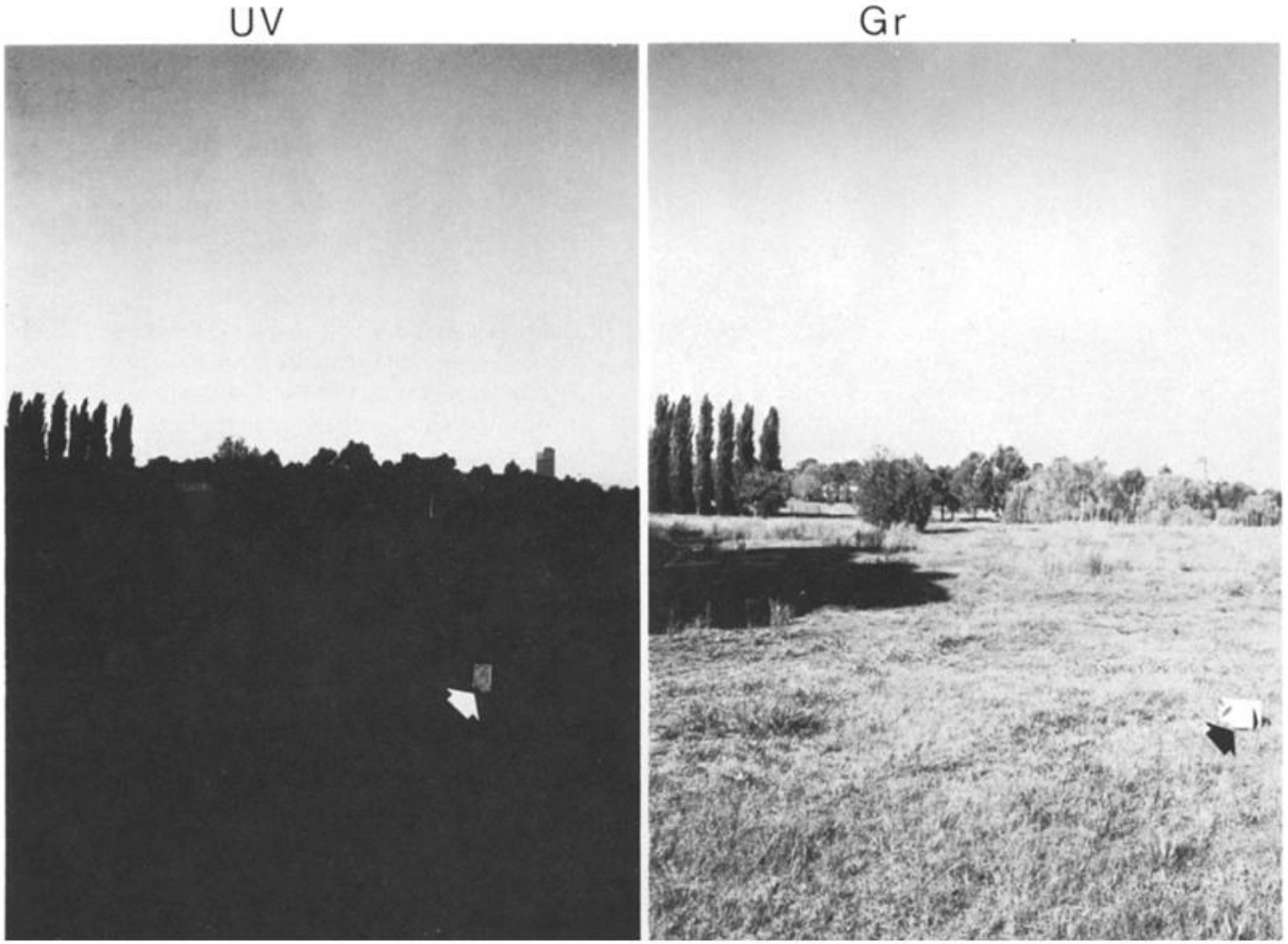

Wilson (*J Comp Physiol*, 1978)

The locust flight simulator

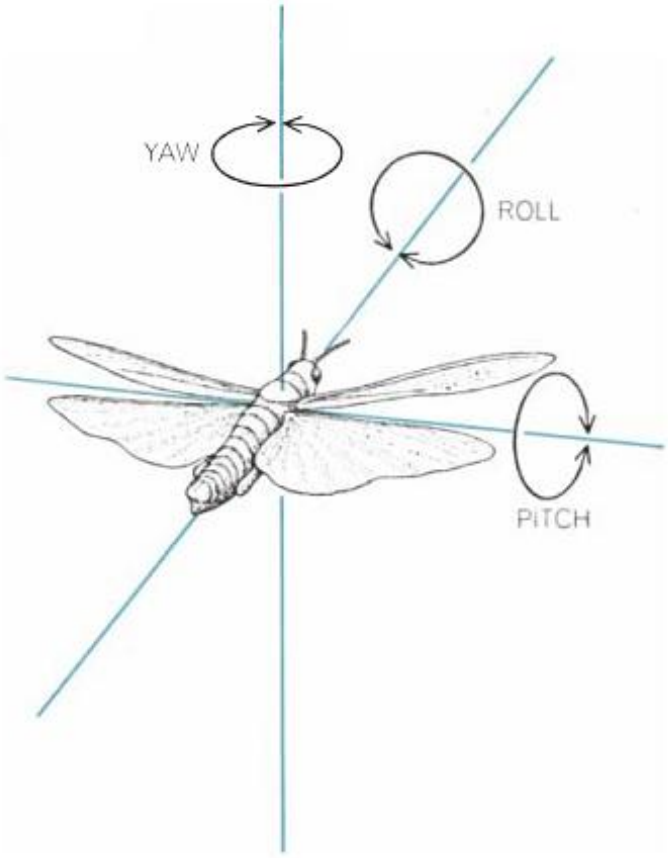

Camhi (*Sci Am*, 1971)

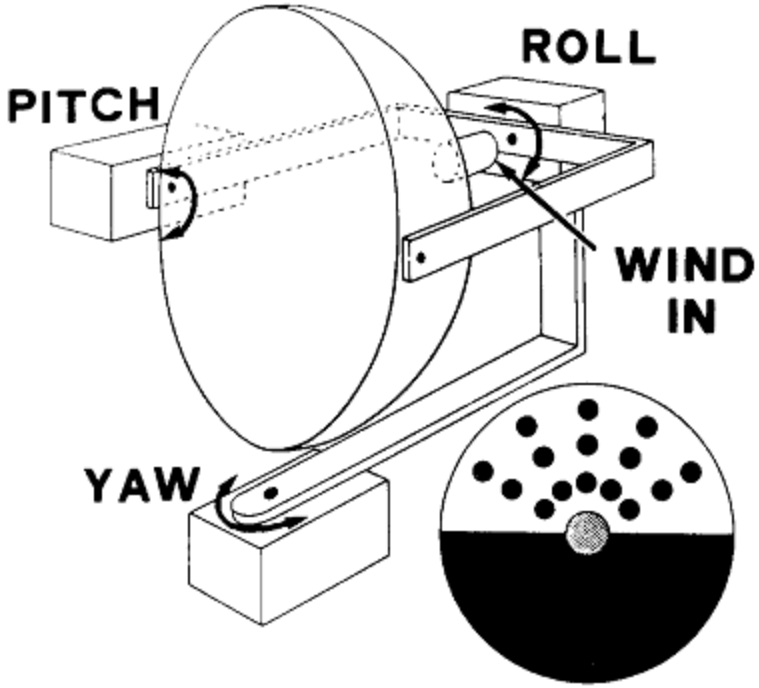

Rowell & Reichert (*J Comp Physiol A*, 1986)

Three deviation-detecting neurons (DDNs)

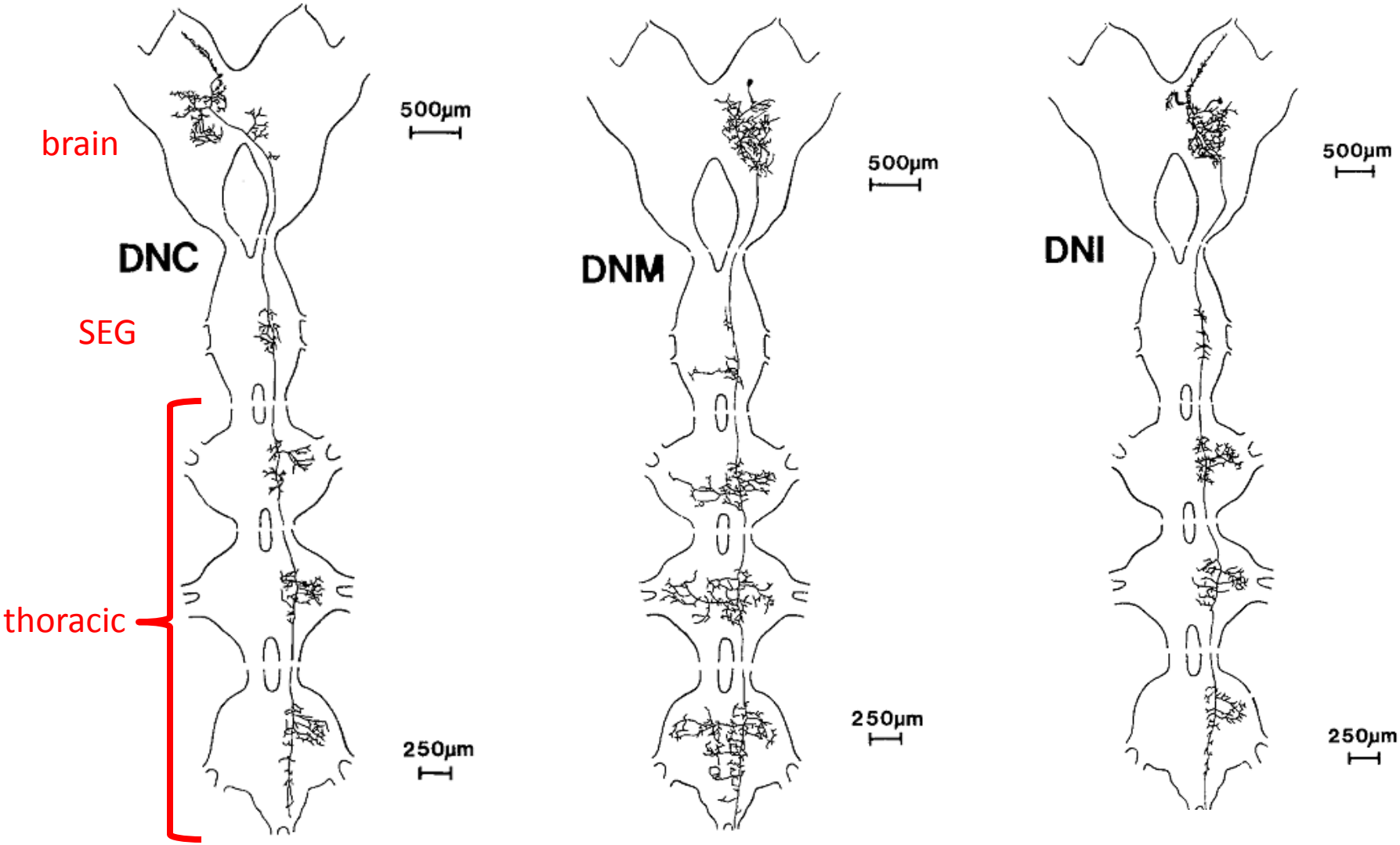

Griss & Rowell (*J Comp Physiol A*, 1986)

DDNs responds to compound eye input

Small deviation

Large deviation

Decrease in deviation

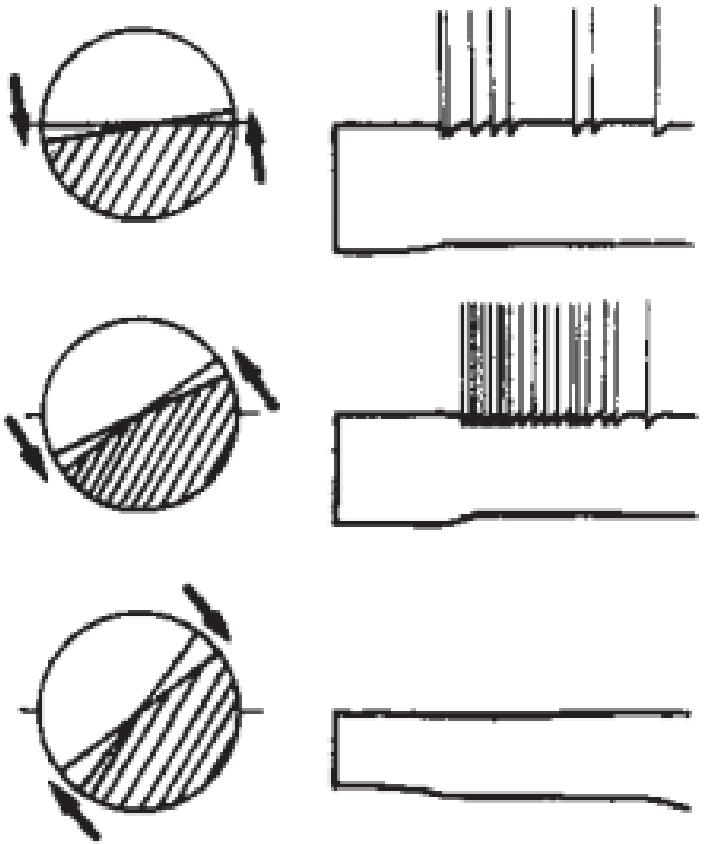

Reichert et al. (*Nature*, 1985)

DDN also responds to combination of roll and wind

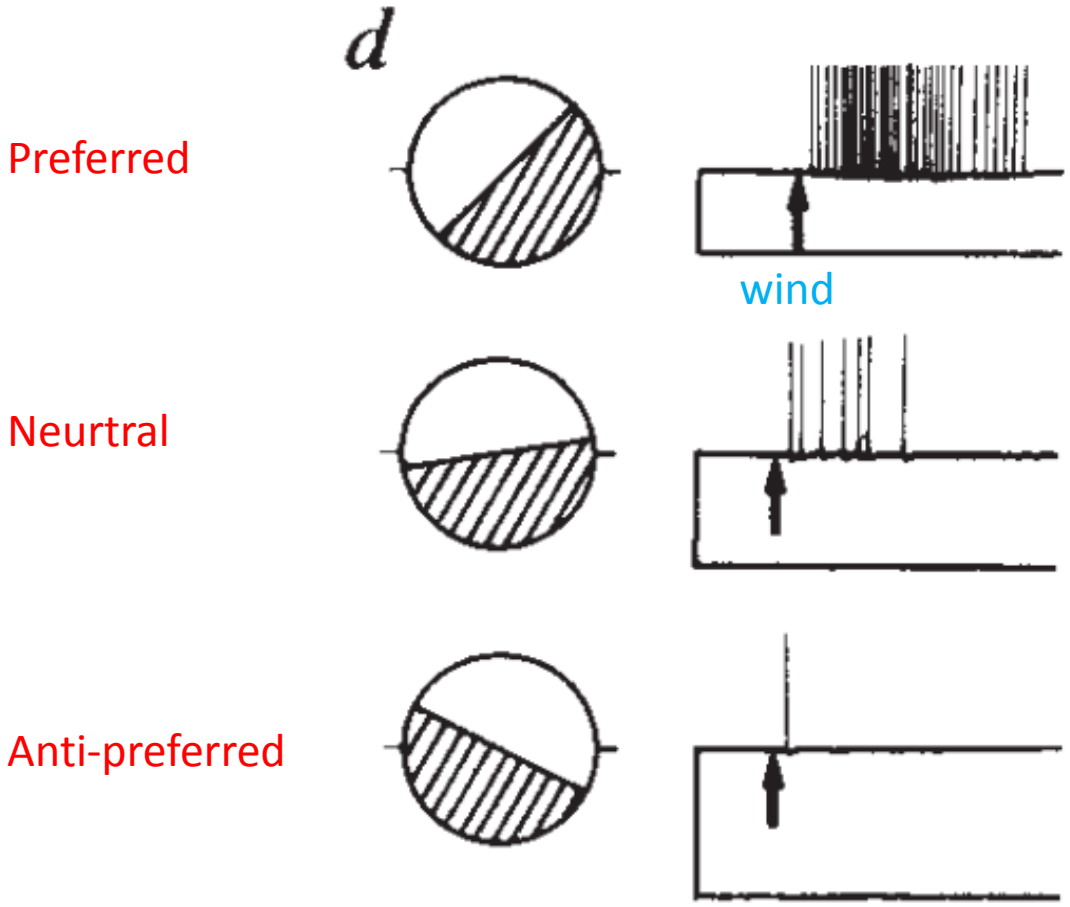

Reichert et al. (*Nature*, 1985)

Ocellar input modulates visual response

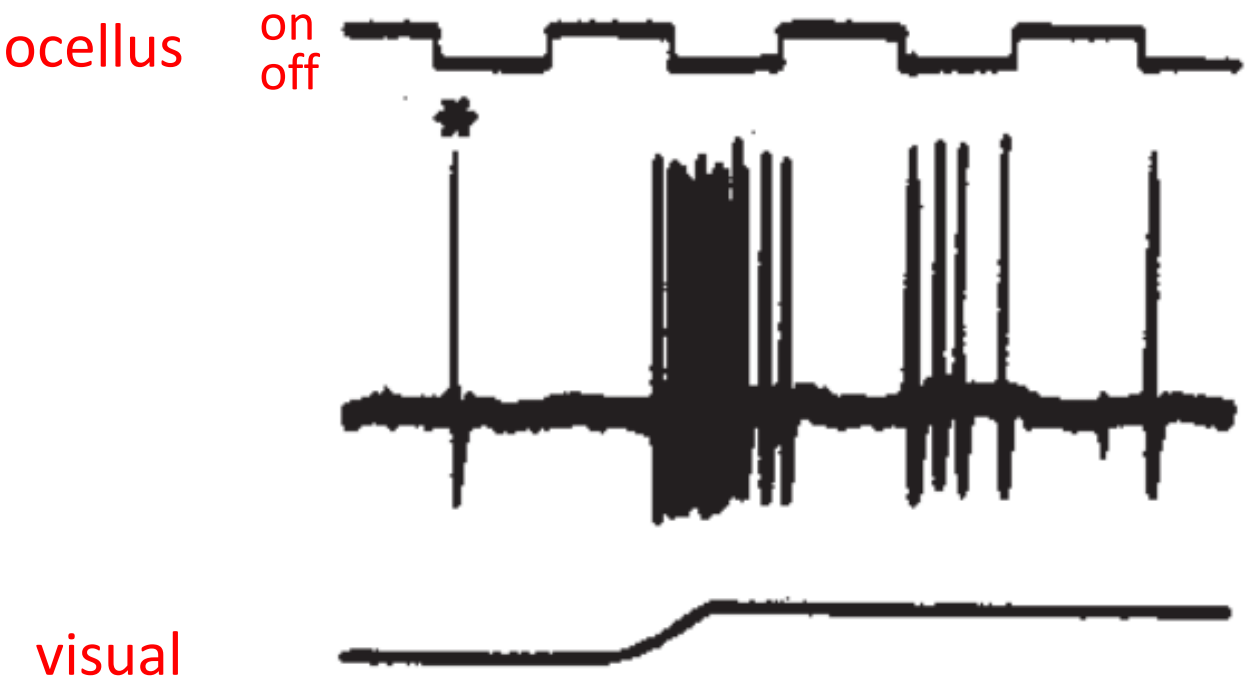

Roll to the right -> darkening of the right ocellus

Reichert et al. (*Nature*, 1985)

Thoracic interneuron (TIN)

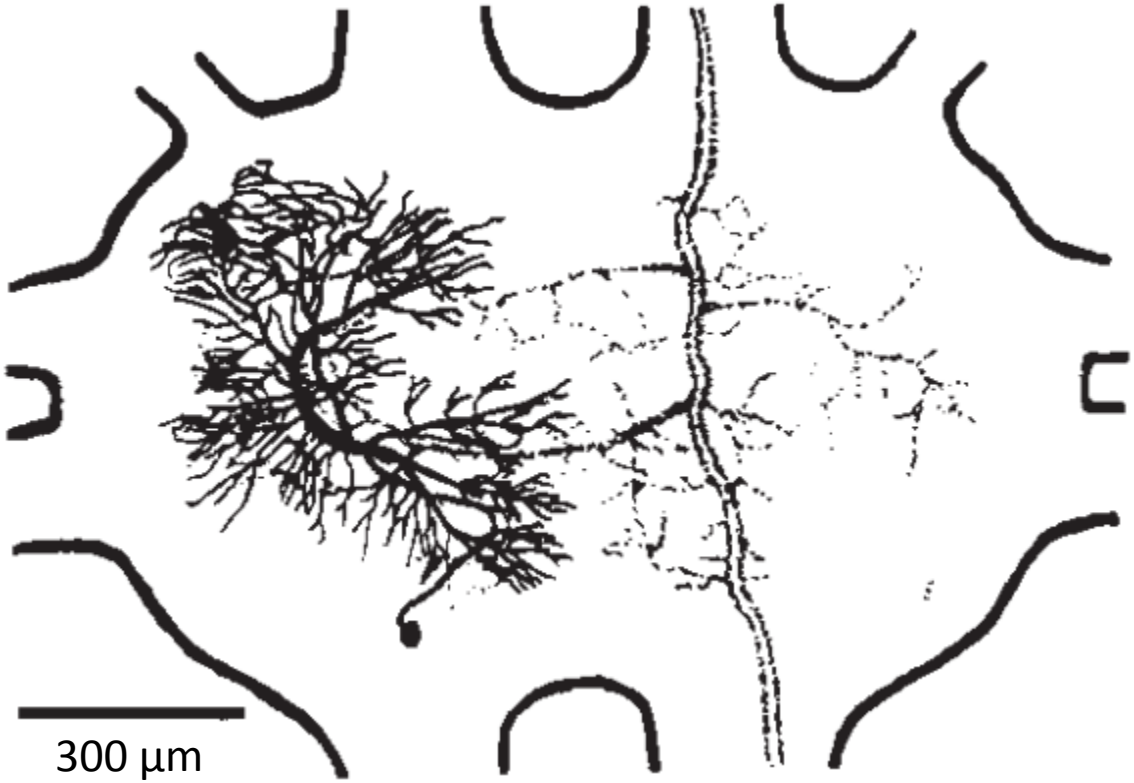

Mesothoracic ganglion

DDN output is not transmitted outside flight

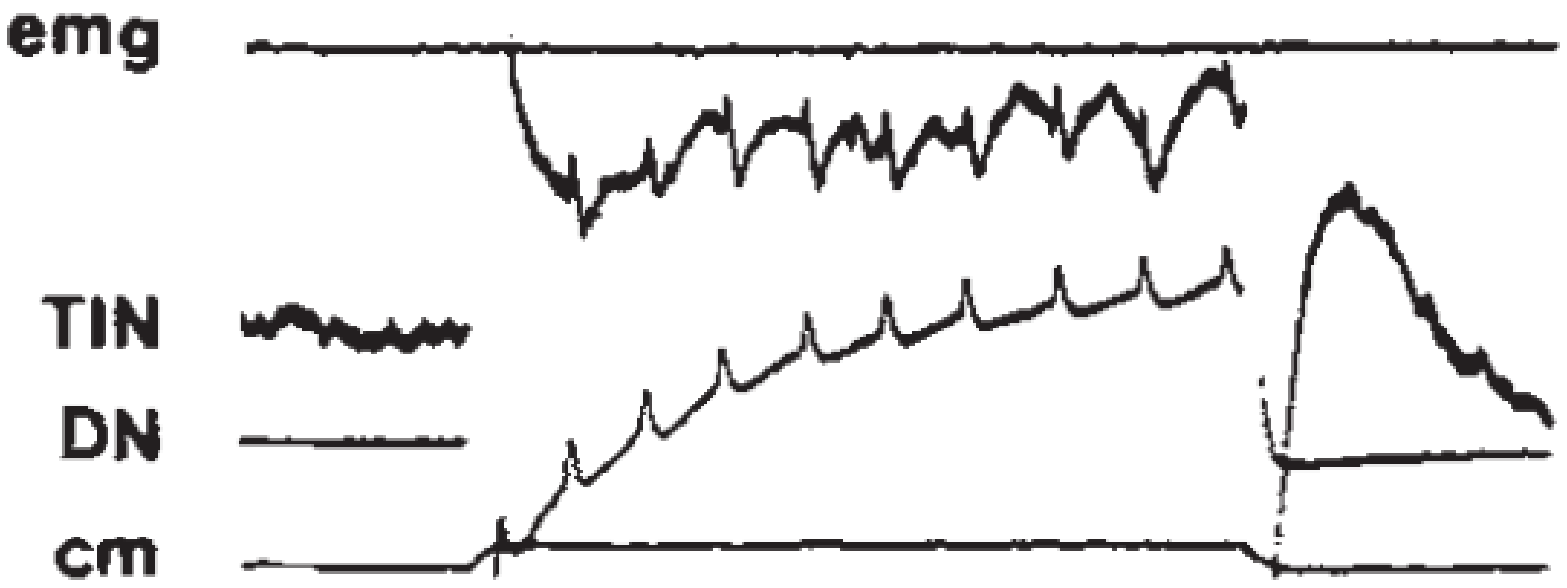

DDN spikes only lead to small EPSPs in TIN.

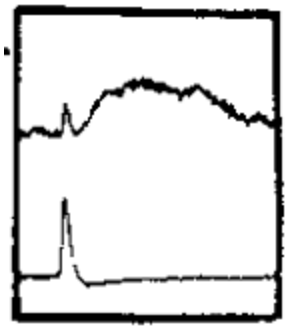

DDN -> TIN is phase dependent!

Depressor phase

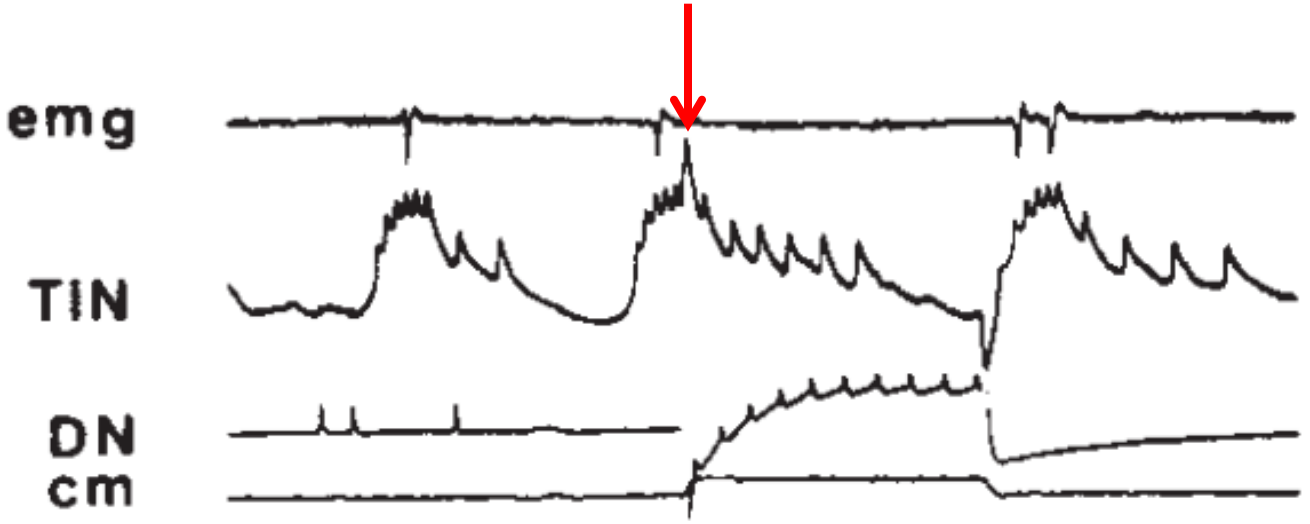

Elevator phase

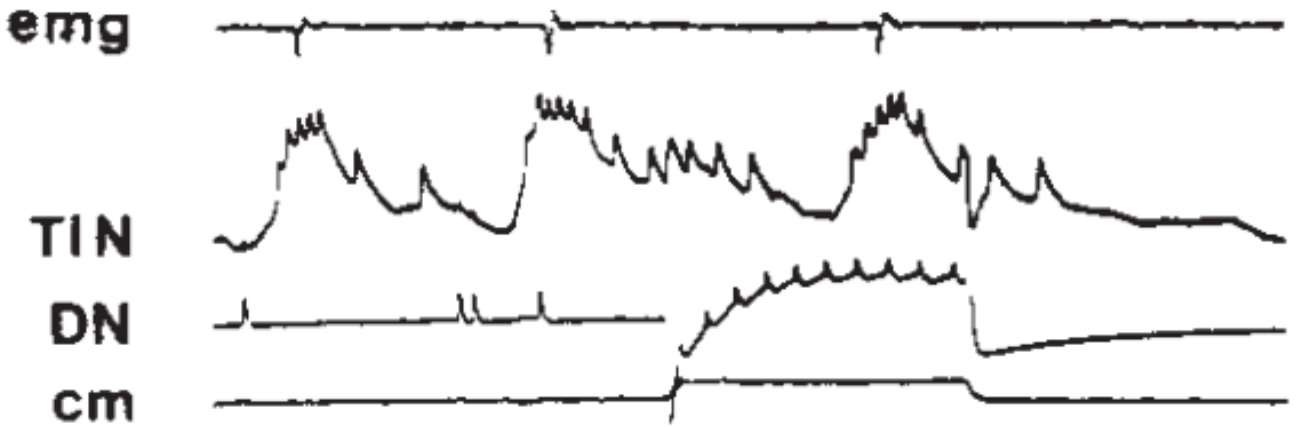

The anatomy of TCG

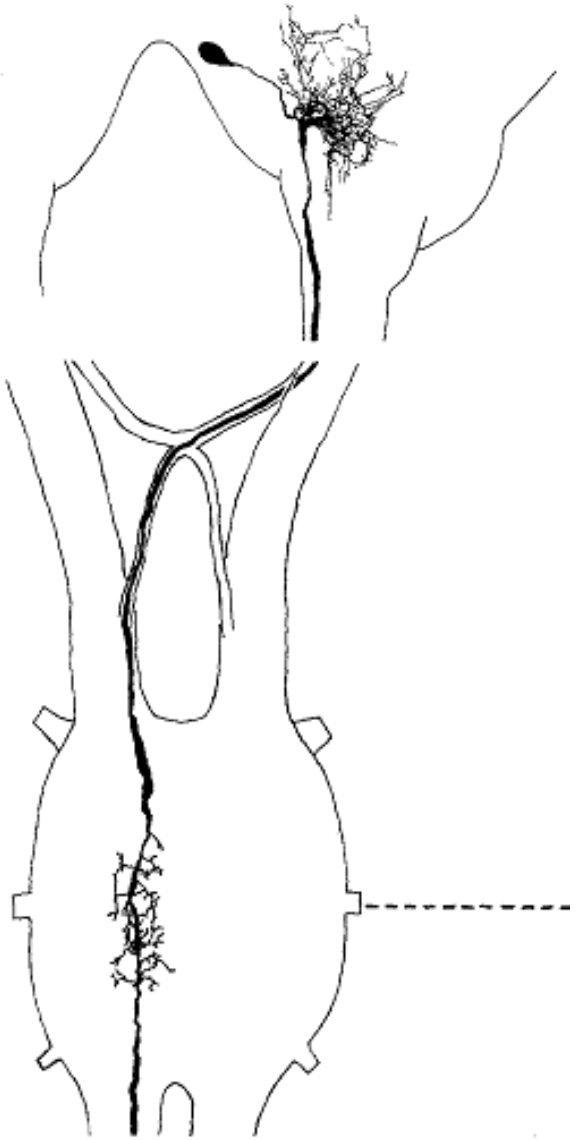

Bacon & Tyrer (*J Comp Physiol A*, 1978)

TCG receives inputs from wind-hair neurons

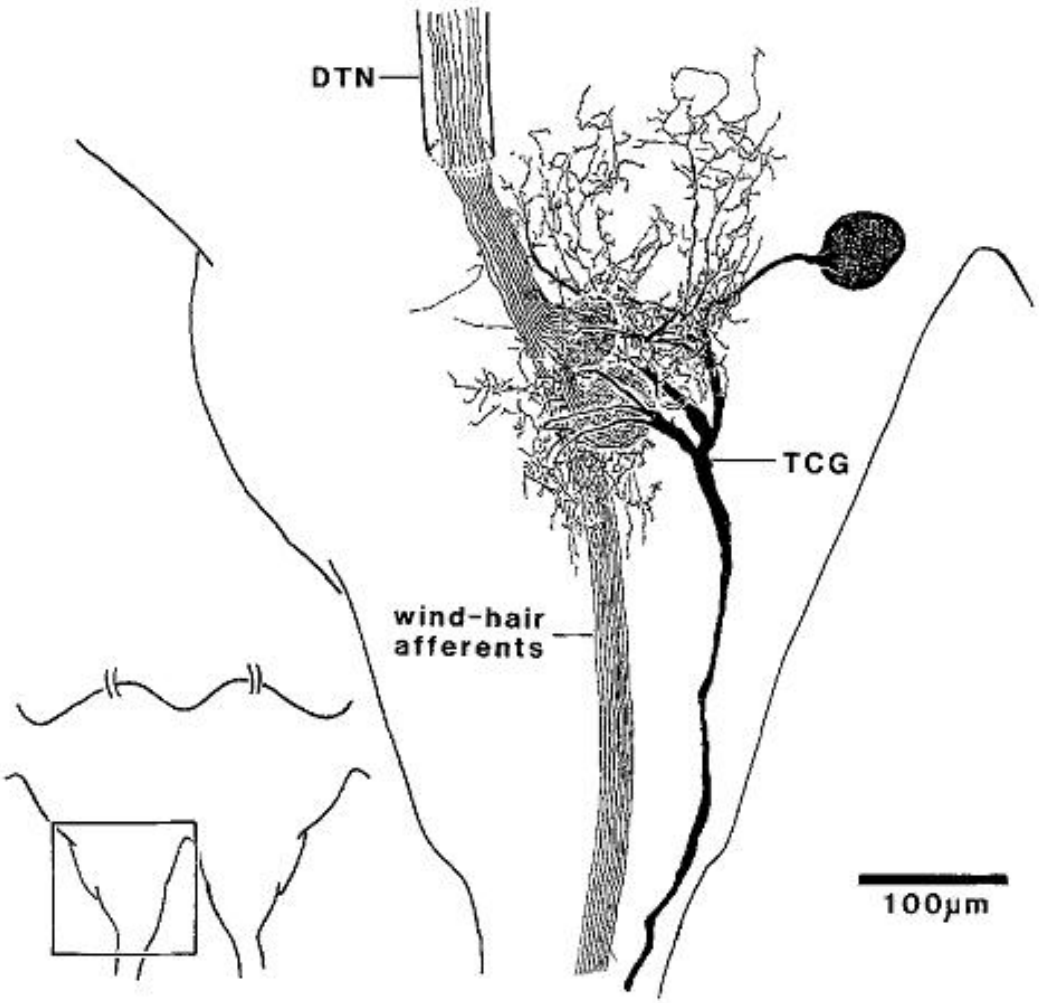

Fig. 2. Drawing of the TCG in the brain. *Insert* shows that region of the brain depicted in the figure. The TCG is seen from the dorsal side in relation to the afferent fibres from the wind hairs. It has its cell body near the crotch of the brain and major region of arborization in the deutocerebrum. Most wind-hair afferent fibres enter the brain dorsally via the dorsal tegumentary nerve (*DTN*) and arborize only in two descrete regions of neuropil (shown *stippled*) before entering the circum-oesophageal connective. These wind-hair output arborizations occur within the dendritic extent of the TCG

Bacon & Möhl (*J Comp Physiol A*, 1978)

Synaptic connection between wind-hair neurons and TCG

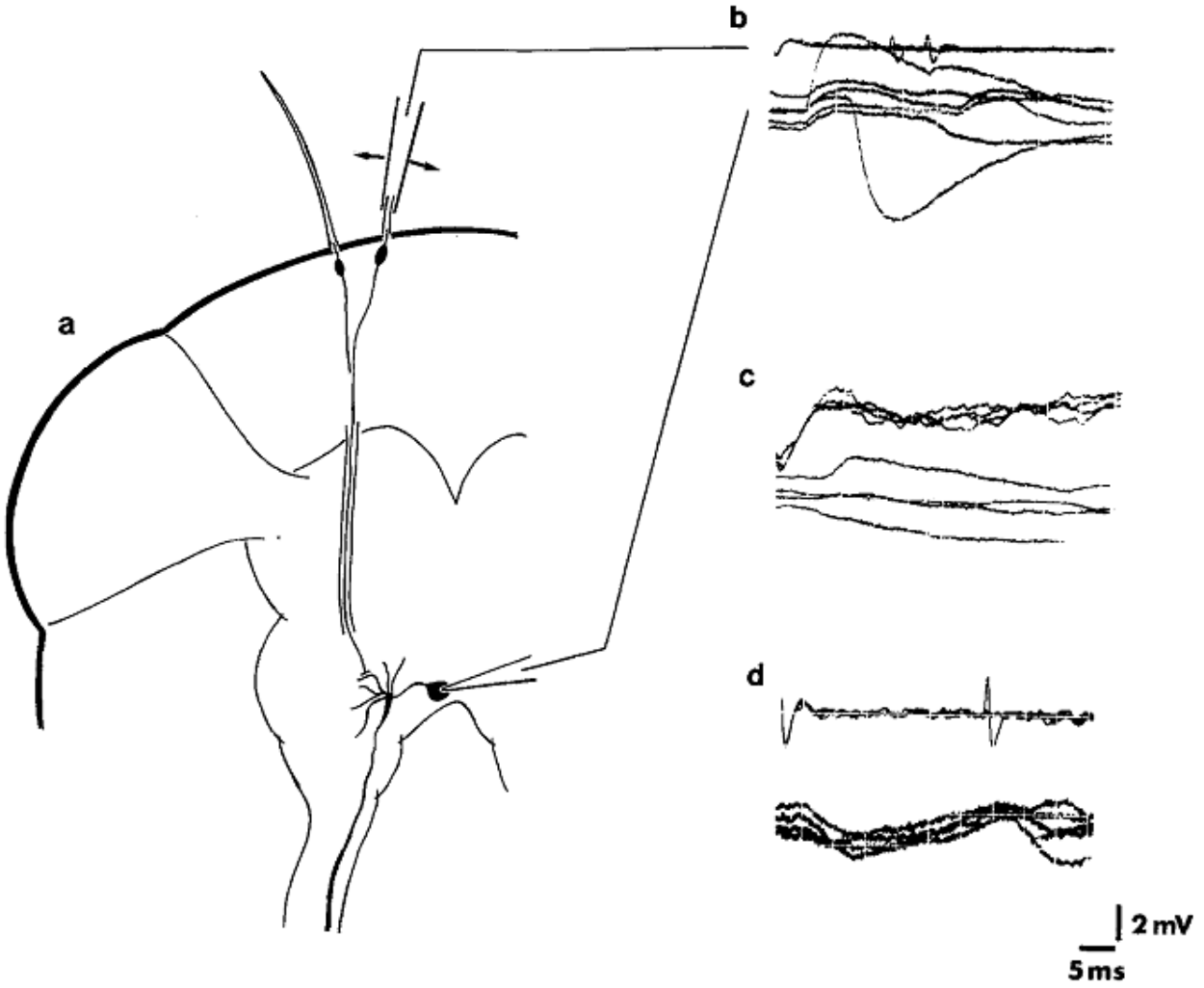

Bacon & Möhl (*J Comp Physiol A*, 1978)

TCG projects to thoracic ganglia

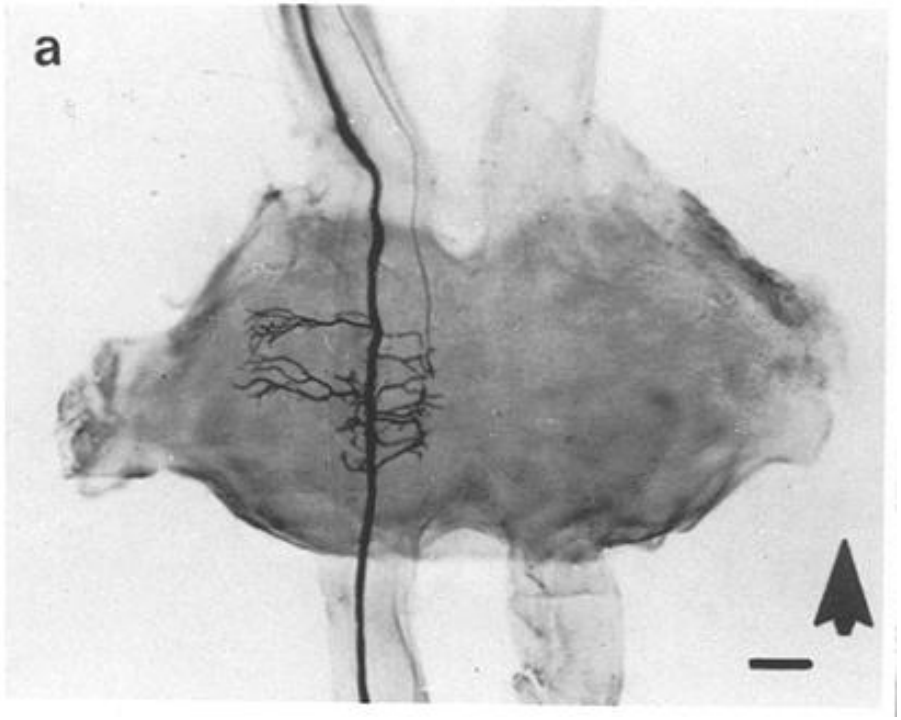

Bacon & Tyrer (*J Comp Physiol A*, 1978)

Recording from TCG using hook electrodes

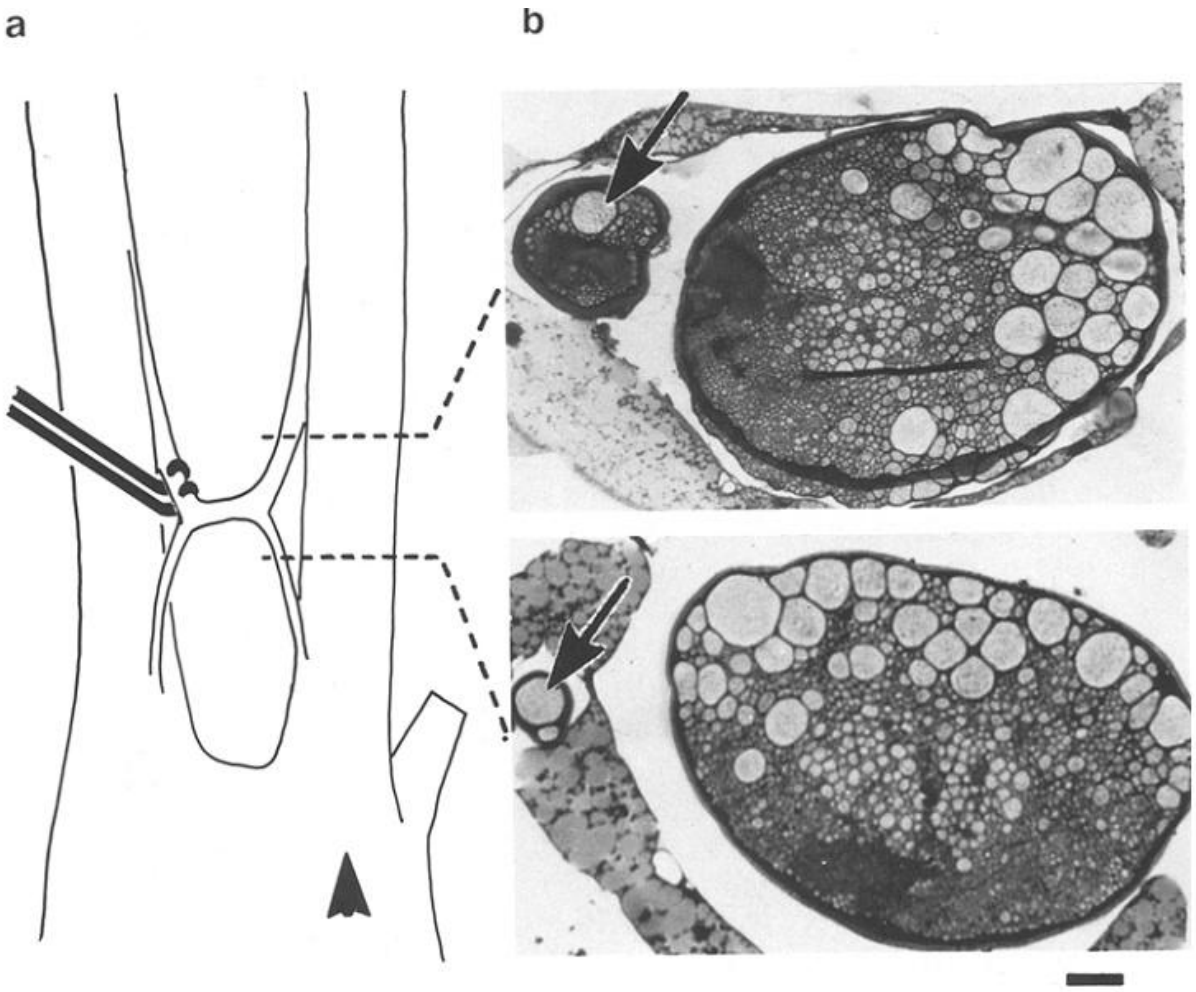

Bacon & Tyrer (*J Comp Physiol A*, 1978)

Response of TCG to wind and light

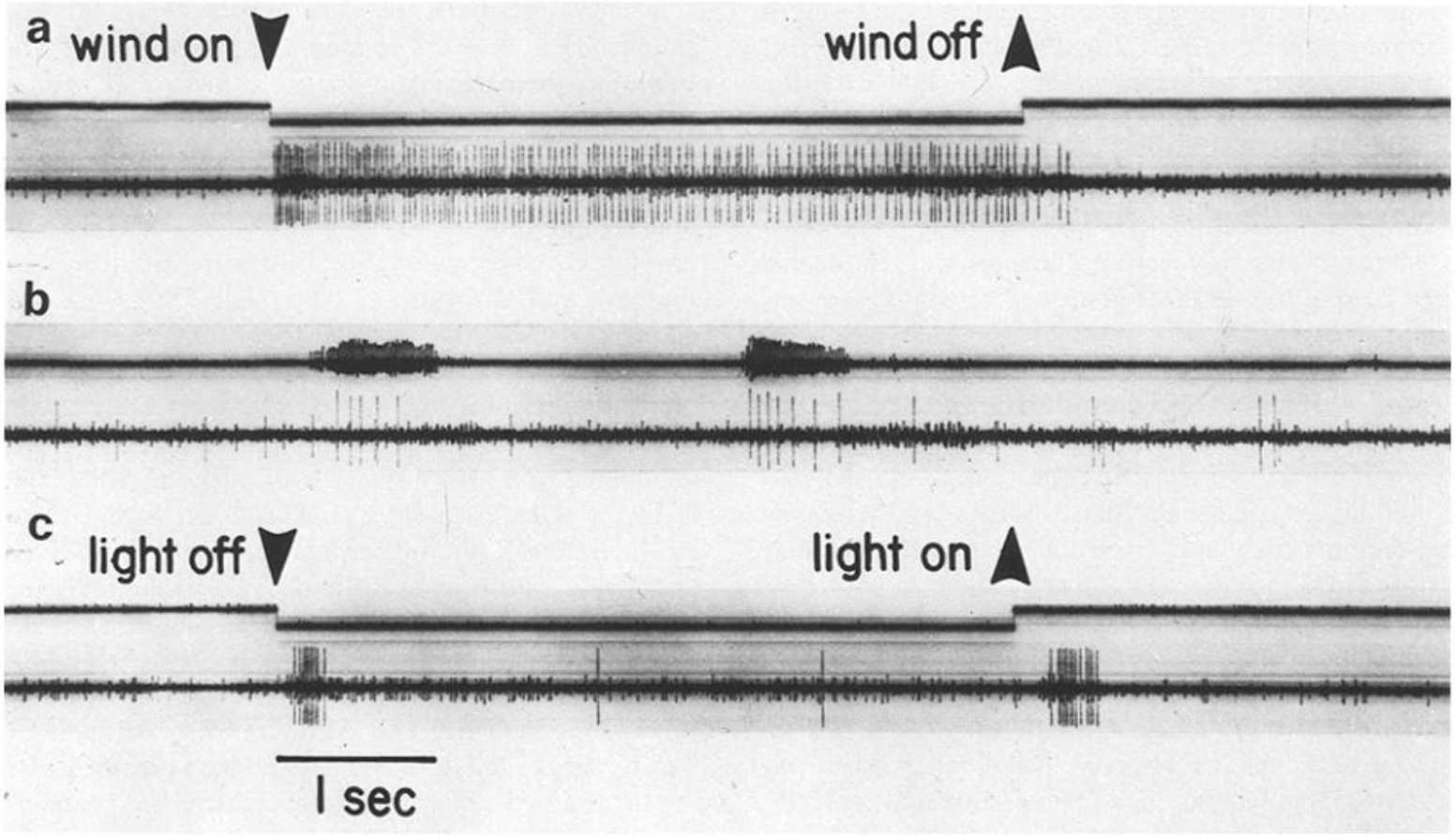

Fig. 6. **a** Responses of the TCG neurone to wind on the head. Upper trace; voltage change as the solenoid operated wind valve was opened and closed. Lower trace; extracellular recorded response from the TCG. Attenuated potentials from the other TCG neurone are also apparent on this trace. **b** Response to movement of an individual hair by displacing it with a pipette electrode recording from the hair. Upper trace; primary sensory response. Lower trace; response of the TCG. **c** Response to switching the microscope lamp on and off. Upper trace; voltage change as the lamp was switched on and off. Lower trace; response of the TCG neurone. The long response latency in this record is due to the slow time course of warming and cooling the lamp filament

Bacon & Tyrer (*J Comp Physiol A*, 1978)